Version of Record: https://www.sciencedirect.com/science/article/pii/S0020740323004848
Manuscript_a5db31e979dd9429c8c8360fe8b2f997

Revised Paper to International Journal of Mechanical Sciences (IJMS-D-23-02063)

Exact Solution of Burst Pressure for Thick-Walled Pipes Using the Flow Theory of Plasticity

Xian-Kui Zhu

Materials Technology and Energy
Savannah River National Laboratory
Aiken, SC 29808
Email address: Xiankui.Zhu@srnl.doe.gov

Abstract: This paper develops an exact solution of burst pressure for defect-free, thick-walled pipes using the flow theory of plasticity in terms of the average shear stress yield criterion (or Zhu-Leis yield criterion). The pipe steel is assumed to obey the power-law strain hardening rule, and large plastic deformation is described by the finite strain theory. On this basis, internal pressure is obtained as a power series function of the effective strains on the inside and outside surfaces of the thick-walled pipe with use of the second Bernoulli numbers. At burst failure, the Zhu-Leis flow solution of burst pressure is determined as a power series solution, and the burst effective strains, the burst effective stresses, and the burst pressure are functions of the diameter ratio (D_o / D_i), strain hardening exponent (n), and ultimate tensile strength (UTS). Similarly, the Tresca and von Mises flow solutions of burst pressure are also determined as a power series solution in terms of the Tresca and von Mises yield criteria. A general closed-from exact solution of burst pressure is then proposed for the three yield criteria, and the results showed that the proposed exact solution matches well with the power series solution for each yield criterion. Moreover, the von Mises flow solution is an upper bound prediction, the Tresca flow solution is a lower bound prediction, and the Zhu-Leis flow solution is an intermediate prediction that agrees well with the finite element analysis results of burst pressure for thick-walled pipes. Two datasets of full-scale burst tests are then utilized to evaluate and validate the proposed flow solutions of burst pressure for both thin and thick-walled pipes.

Keywords: burst pressure, thick-walled pipe, power-law strain hardening, flow theory of plasticity, von Mises yield criterion, Tresca yield criterion, Zhu-Leis yield criterion

1. Introduction

Transmission pipelines are the critical infrastructure of a nation and used as an efficient and safe vehicle to transport large volumes of crude oil, natural gas, refined petroleum products, or hazardous liquids over long distances. In general, transmission pipelines are constructed from carbon steel pipes and can range in size from several inches to several feet in diameter [1]. Most transmission pipelines are large diameter, thin-walled pipes with a diameter to wall thickness ratio $D/t \geq 20$ [2, 3], although there are many applications where pipes or tubes have small diameters and thick walls with a ratio of $D/t < 20$ [3-5]. Because of high internal pressure, these pipelines are potentially dangerous to human life and the environment. Accordingly, pipeline structural integrity becomes extremely important for pipeline systems and has attracted broad attentions [2-10]. To ensure the safe operation of pipelines, a pipeline design and integrity management plan requires the accurate yield and burst strengths of the pipes to be available so

that the maximum operating pressure will be less than the maximum load-bearing capacity or burst pressure of the pipes. Therefore, an accurate burst pressure prediction model is essentially needed for the pipeline design and management.

Extensive theoretical, numerical and experimental investigations have been performed over the past century in order to accurately estimate burst pressure of cylindrical pressure vessels or pipes, and many analytical and empirical prediction models were developed for predicting burst pressure of defect-free pipes with internal pressure. For thick-walled pressure vessels, Hamada et al. [4] and Christopher et al. [11, 12] presented a good technical review of burst pressure models, while for thin-walled line pipes, Zhu and Leis [13] and Law and Bowie [14] evaluated available burst pressure models. Recently, Zhu [8, 15] performed a comparative study on the traditional strength criteria versus the modern plastic flow criteria used in the pressure vessel design and analysis, Wang et al. [7] evaluated a set of burst prediction models using their burst test data for structural steels exhibiting a yield plateau, Sun et al. [9] reevaluated existing burst pressure models for large diameter, thin-walled pipelines in various grades, and Oh et al. [16] proposed a new numerical model for thin-walled pipes from the finite element analysis (FEA).

The above-noted literature reviews [4-15] determined that most of available burst prediction models were developed from either a simple analysis using a strength theory in terms of ultimate tensile stress (UTS) and/or yield strength (YS), or using an empirical curve fit of experimental data for one or more specific steels. It was concluded that no single model can provide an accurate prediction of burst pressure for all ductile steels, or has been broadly accepted by the industry. As a result, the simple Barlow strength formula [17] remains the basic design model for developing regulation rules in both the American Society of Mechanical Engineers (ASME) Boiler and Pressure Vessel Codes (BPVC) [18] and ASME B31.3 Codes [19], where ASME BPVC is typically used in the pressure vessel industry, and ASME B31.3 is commonly used in the pipeline industry. However, these code models did not consider the effect of plastic flow response or strain hardening rate on burst strength of end-capped pressure vessels or pipes.

In order to consider the plastic flow effect on burst pressure, Cooper [20] and Svensson [21] adopted the flow theory of plasticity and obtained the von Mises flow solution of burst pressure for thin-walled pressure vessels in the end-capped conditions. Similarly, Weil [22] and Hillier [23] performed a tensile plastic instability analysis of thin-walled tubes and obtained the same result. Using experimental data, Kiefner et al. [24] and Stewart and Klever [25] demonstrated that the von Mises flow solution obtained by Cooper [20] and Svensson [21] can describe the effect of strain hardening rate on burst pressure, but significantly overestimated the burst test data for thin-walled line pipes in various steels. Due to this reason, Stewart and Klever [25] adopted the Tresca flow theory of plasticity and obtained the Tresca flow solution of burst pressure for thin-walled pipes. These authors found that the von Mises flow solution provided an upper bound of burst pressure data, while the Tresca flow solution provided a lower bound of burst pressure data. The averaged result of these two bound solutions provides a good fit to the burst test data, where both von Mises and Tresca solutions obtained from the flow theory of plasticity are functions of the UTS, n and D/t ratio. So motivated, Zhu and Leis [26, 27] developed a new multi-axial plastic yield theory that was referred to as the average shear stress yield criterion, or simply the Zhu-Leis criterion. Then, an intermediate flow solution of burst pressure was developed for thin-walled pipes, and various experiments showed that the Zhu-Leis flow solution agrees with well full-scale burst test data on average for a wide range of pipeline steels from Grade A to X120. Many other researchers [28-31] also validated the Zhu-Leis flow solution using different full-scale burst test datasets for various pipeline steels. All validations

demonstrated that the Zhu-Leis flow solution provides a reliable, accurate prediction of burst pressure for defect-free, thin-walled line pipes. Recently, the average shear stress yield theory has been extended to determine burst pressure for thin-walled pipe elbows [32], cylindrical shells in dynamic conditions [33], ductile PVC pipes [34], and offshore tubular casings [35, 36].

However, the above-noted Zhu-Leis flow solution was developed for thin-walled pipes, but not applicable for thick-walled pipes because the wall thickness effect on burst pressure was not considered. The literature review determined that an exact theoretical solution of burst pressure does not exist for thick-walled pipes due to the complexity of mathematical calculations. In the 1950s, Faupel [37, 38] conducted a large set of burst pressure tests using small diameter, thick-walled tubes in the capped end conditions, and proposed an empirical burst model based on their burst test data to predict burst strength of thick-walled tubes. Svensson [21] performed a theoretical study on burst pressure of thick-walled cylinders based on the von Mises flow theory. However, this author failed to develop an exact theoretical solution because of a complicated integration in the mathematical derivation, and thus obtained an approximate closed-form solution of burst pressure for thick-walled pressure vessels. Nevertheless, up to date, the approximate Svensson solution has obtained extensive applications [39-42] in structural design and strength analysis of intermediate thick-walled pressure vessels because of its fair agreement with full-scale test data for an intermediate D/t ratio in the range of $10 < D/t < 20$. However, for small diameter, thick-walled tubes or pipes with a small D/t ratio in the range of $2 < D/t < 5$, the difference between the Svensson solution and full-scale burst test data can be significantly large, up to 15%, see Section 4.1 or Reference [51] for detailed comparisons. As a result, a more accurate exact solution of burst pressure for thick-walled pipes is still needed in the pressure vessel and pipeline industry.

This paper aims to develop an exact solution of burst pressure for defect-free, thick-walled pipes with capped ends using the flow theory of plasticity in terms of the average shear stress yield criterion (or Zhu-Leis yield criteria). It is assumed that the pipe material obeys the power-law strain hardening rule, and the finite strain theory is adopted to describe large plastic deformation. On this basis, internal pressure is obtained as a power series function of the effective strains on the inside and outside surfaces of the thick-walled pipe with use of the second Bernoulli numbers. At burst failure, the Zhu-Leis flow solution of burst pressure is determined as a power series solution, and the burst effective strains, the burst effective stresses, and the burst pressure are a function of the diameter ratio (D_o / D_i), strain hardening exponent (n), and ultimate tensile strength (UTS). In the similar manner, the Tresca and von Mises flow solutions of burst pressure are also determined as a power series solution in terms of the Tresca and von Mises yield criteria, respectively. A general closed-from exact solution of burst pressure is then proposed for the three yield criteria, and the results showed that the proposed exact solution matches well with the power series solution for each yield criterion. Moreover, the von Mises flow solution is an upper bound prediction, the Tresca solution is a lower bound prediction, and the Zhu-Leis flow solution is an intermediate prediction that agrees well with the FEA results of burst pressure for thick-walled pipes. Finally, two datasets of full-scale burst tests are employed to evaluate and validate the proposed flow solutions of burst pressure for both thin and thick-walled pipes.

2. Existing burst prediction models for thick-walled pipes

In the 1950s and 1960s, there were many valuable burst pressure tests conducted for small diameter, thick-walled tubes (i.e., D/t < 20) in various structural steels by different investigators [37-38, 43-44]. Many empirical burst pressure models were then developed for thick-wall tubes in the capped-end conditions, as reviewed by Hamada et al. [4] and Christopher et al. [11]. Four of these burst pressure models are often used in the pressure vessel industry.

2.1. Turner burst pressure model

$$P_b = S_{uts} \ln\left(\frac{D_o}{D_i}\right) \tag{1}$$

where P_b is burst pressure, S_{uts} is the engineering value of UTS of the pipe steel, D_o is the outside diameter (OD), and D_i is the inside diameter (ID) of the pipe. This burst pressure solution in Eq. (1) was obtained by Turner [45] in 1910 using the Tresca strength theory in terms of the UTS for thick-walled pressure cylinders.

2.2. Nadai burst pressure model

$$P_b = \frac{2}{\sqrt{3}} S_{uts} \ln\left(\frac{D_o}{D_i}\right) \tag{2}$$

This burst pressure solution in Eq. (2) was obtained by Nadai [46] in 1931 using the von Mises strength theory [35] in terms of the UTS for thick-walled tubes.

2.3. Faupel burst pressure model

$$P_b = \frac{2}{\sqrt{3}} S_{ys} \left(2 - \frac{S_{ys}}{S_{uts}}\right) \ln\left(\frac{D_o}{D_i}\right) \tag{3}$$

where S_{ys} is the yield stress (YS) of the pipe. This burst prediction formula in Eq. (3) is an empirical model that was proposed by Faupel [37] in 1956 based on his burst test data, the von Mises yield strength and the von Mises ultimate tensile strength of failure pressure for thick-walled tubes.

2.4. Svensson burst pressure model

$$P_b = \left(\frac{0.25}{n+0.227}\right)\left(\frac{e}{n}\right)^n S_{uts} \ln\left(\frac{D_o}{D_i}\right) \tag{4}$$

where e = 2.71828 is the Euler's number and n is the strain hardening exponent of ductile steels. This burst pressure model in Eq. (4) is an approximate solution for thick-walled pressure vessels that was obtained by Svensson [21] in 1958 using the von Mises flow theory of plasticity that considered the plastic flow response of steel pipes.

2.5. Three flow solutions of burst pressure for thin-walled pipes

In order to consider the plastic flow effect as did by Svensson [21], Zhu and Leis [26, 27] investigated burst pressure of large diameter, thin-walled pipes with a ratio of D/t ≥ 20 using the flow theory of plasticity within the large deformation framework. For a power-law hardening steel, these authors developed the following flow solutions of burst pressure for thin-walled pipes with regard to the Tresca, von Mises and Zhu-Leis criteria as:

$$P_b = \left(\frac{1}{2}\right)^{n+1} \frac{4t}{D-t} S_{uts}, \qquad \text{for Tresca yield criterion} \tag{5}$$

$$P_b = \left(\frac{1}{\sqrt{3}}\right)^{n+1} \frac{4t}{D-t} S_{uts}, \qquad \text{for von Mises yield criterion} \tag{6}$$

$$P_b = \left(\frac{2+\sqrt{3}}{4\sqrt{3}}\right)^{n+1} \frac{4t}{D-t} S_{uts}, \qquad \text{for Zhu-Leis yield criterion} \tag{7}$$

where D-t is the mean diameter (MD) of the pipe, D is the OD of the pipe, and strain hardening exponent *n* is measured from a simple tensile test or estimated from the YS and UTS. Zhu and Leis [47] provided two simple equations to estimate n from the YS defined at the 0.2% offset strain or the 0.5% total strain.

For an elastic-perfectly plastic material or n ≈ 0, Equations (5) – (7) reduces to the strength solution of burst pressure in terms of the Tresca, von Mises and Zhu-Leis yield criteria [15]. In particular, using the OD, the Tresca strength solution of burst pressure is often referred to as the Barlow strength in the pipeline industry:

$$P_b = \frac{2t}{D} S_{uts} \tag{8}$$

Comparison of Eq. (8) with Eq. (1) shows that the Tresca strength solution has a different geometrical term, but the same material term for a thick-walled pipe compared to a thin-walled pipe. The same observation is made for the von Mises Strength solution for a thick-walled pipe compared to a thin-walled pipe. If this observation holds truly for a power-law hardening material, the Svensson burst solution in Eq. (4) for a thick-walled pipe and the von Mise flow solution in Eq. (6) for a thin-walled pipe should have the same material term. However, the material terms in these two equations are considerably different. The root cause is that the Svensson model Eq. (4) is an approximate result, but not an exact solution for thick-walled pipes. This motivates the present work to adopt the flow theory of plasticity to strictly develop a more accurate, exact theoretical solution of burst pressure for thick-walled pipes.

3. Exact solutions of burst pressure for thick-walled pipes

3.1. Stress-strain law

For a power-law strain hardening material, the true stress, σ, and the logarithmic strain, ε, in the uniaxial tensile test obeys the following power-law stress-strain relationship [27]:

$$\sigma = K\varepsilon^n \quad \text{or} \quad \frac{\sigma}{\sigma_{uts}} = \left(\frac{\varepsilon}{n}\right)^n \tag{9}$$

$$K = S_{uts}\left(\frac{e}{n}\right)^n \tag{10}$$

where K is a strength coefficient of the material, and σ_{uts} is the true UTS that is related to the engineering UTS as $\sigma_{uts} = e^n S_{uts}$. At the UTS, the true strain $\varepsilon_{uts} = n$.

In general, a simple relationship does not exist between internal pressure, stress, and strain for a thick-walled pipe in an elastic-plastic deformation due to plastic flow response and large strain effects [48]. This work adopts the power-law strain hardening rule in Eq. (9), the flow theory of plasticity, and the finite strain theory to characterize stresses and strains in a thick-walled pipe for pipeline carbon steels that obey the power-law strain hardening rule.

3.2. Effective stress and effective strain for the average shear stress yield criterion

For a long thick-walled pipe with capped ends, experiments [37] showed that the axial strain is very small and can be neglected (i.e., $\varepsilon_{zz} = 0$). The three principal stresses in a thick-walled pipe are radial stress σ_{rr}, hoop stress $\sigma_{\theta\theta}$, and axial stress σ_{zz}, while the three principal strains are radial strain $\varepsilon_{rr} \neq 0$, hoop strain $\varepsilon_{\theta\theta} \neq 0$, and axial strain $\varepsilon_{zz} = 0$. In the large plastic deformation near plastic collapse, the material becomes incompressible (i.e., the Poisson's ratio $\nu = 0.5$). In these conditions, the following relations [11, 21] were obtained:

$$\varepsilon_{rr} = -\varepsilon_{\theta\theta} \tag{11}$$

$$\sigma_{zz} = \frac{1}{2}(\sigma_{rr} + \sigma_{\theta\theta}) \tag{12}$$

For an elastic-plastic deformation, the plastic flow theory in terms of the average shear stress (i.e., Zhu-Leis) yield criterion [27] determines the effective stress, σ_A, and effective strain, ε_A:

$$\sigma_A = \frac{1}{2+\sqrt{3}}\left(\sqrt{3}\sigma_T + 2\sigma_M\right) = \frac{2\sqrt{3}}{2+\sqrt{3}}(\sigma_{\theta\theta} - \sigma_{rr}) \tag{13a}$$

$$\varepsilon_A = \frac{1}{2}(\varepsilon_T + \varepsilon_M) = \frac{2+\sqrt{3}}{2\sqrt{3}}\varepsilon_{\theta\theta} \tag{13b}$$

where σ_T and ε_T are the effective stress and effective strain for the Tresca yield condition:

$$\sigma_T = \sigma_{\theta\theta} - \sigma_{rr} \tag{14a}$$

$$\varepsilon_T = \varepsilon_{\theta\theta} \tag{14b}$$

and σ_M and ε_M are the effective stress and effective strain for the von Mises yield condition:

$$\sigma_M = \frac{\sqrt{3}}{2}(\sigma_{\theta\theta} - \sigma_{rr}) \tag{15a}$$

$$\varepsilon_T = \frac{2}{\sqrt{3}}\varepsilon_{\theta\theta} \tag{15b}$$

3.3. Governing equation

Consider an infinitesimal, differential element in a thick-walled pipe subjected to internal pressure, as shown in Fig. 1, where (X, Y) is the Cartesian rectangular coordinate system, (r, θ) is the polar coordinate system, and z denotes the axial direction for both coordinate systems.

For a thick-walled pipe, D/t < 20, or the diameter ratio $\kappa = D_o / D_i > 1.1$. Initially before loading, the differential element in the undeformed configuration lies at a point (r, θ) with a radial increment, dr, and an angular increment, dθ. Because of axial symmetry, the pipe has no hoop displacement but only radial displacement that is denoted as *u*. During loading, the pipe expands,

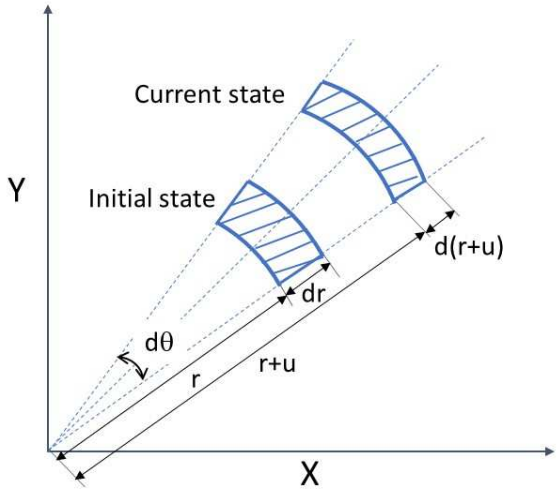

Figure 1. Illustration of a differential element in a thick-walled pipe.

and so the differential element moves outward to a new point $(r + u, \theta)$, and the radial increment becomes $d(r + u)$. The equation of stress equilibrium in the radial direction is expressed as:

$$(r+u)\frac{d\sigma_{rr}}{d(r+u)} = \sigma_{\theta\theta} - \sigma_{rr} \tag{16}$$

where the instantaneous radial stress σ_{rr} and the instantaneous hoop stress $\sigma_{\theta\theta}$ of the differential element in the pipe are the Cauchy stresses defined in the deformed configuration.

Since large plastic deformation is involved, the finite strain theory determines the radial and hoop logarithmic strains, respectively as:

$$\varepsilon_{rr} = ln\left(1 + \frac{du}{dr}\right) \tag{17a}$$

$$\varepsilon_{\theta\theta} = ln\left(1 + \frac{u}{r}\right) \tag{17b}$$

By eliminating the radial displacement *u* from Eqs. (17a) and (17b), the following strain compatibility equation is obtained in reference to the instantaneous radius, *r*+*u*:

$$(r+u)\frac{d\varepsilon_{\theta\theta}}{d(r+u)} = 1 - e^{\varepsilon_{\theta\theta}-\varepsilon_{rr}} \tag{18}$$

Using Eqs. (13a) and (9), the equation of stress equilibrium in Eq. (16) becomes:

$$(r+u)\frac{d\sigma_{rr}}{d(r+u)} = \left(\frac{2+\sqrt{3}}{2\sqrt{3}}\right) S_{uts}\left(\frac{e}{n}\right)^n \varepsilon_A^n \tag{19}$$

From Eqs. (13b), the strain compatibility equation (18) becomes:

$$(r+u)\frac{d\varepsilon_A}{d(r+u)} = \left(\frac{2+\sqrt{3}}{2\sqrt{3}}\right)\left(1 - e^{\frac{4\sqrt{3}}{2+\sqrt{3}}\varepsilon_A}\right) \tag{20}$$

Dividing Eq. (20) by Eq. (19) obtains the following governing equation:

$$\frac{d\sigma_{rr}}{d\varepsilon_A} = \frac{S_{uts}\left(\frac{e}{n}\right)^n \varepsilon_A^n}{1-e^{\frac{4\sqrt{3}}{2+\sqrt{3}}\varepsilon_A}} \tag{21}$$

The thick-walled pipe subjected to internal pressure has the following stress and strain boundary conditions:

- On the ID surface at r = R_i, $\sigma_{rr} = -P$ (22a)
- On the OD surface at r = R_o, $\sigma_{rr} = 0$ (22b)

where $R_i = D_i/2$ is the inside radius, and $R_o = D_o/2$ is the outside radius of the pipe. For convenience of analysis, denote $\varepsilon_A = \varepsilon_1$ on the ID surface, and $\varepsilon_A = \varepsilon_2$ on the OD surface.

With the boundary conditions in Eq. (22), integration of Eq. (21) determines the pressure as:

$$P = S_{uts}\left(\frac{e}{n}\right)^n \int_{\varepsilon_1}^{\varepsilon_2} \frac{\varepsilon_A^n}{1-e^{\frac{4\sqrt{3}}{2+\sqrt{3}}\varepsilon_A}} d\varepsilon_A \tag{23}$$

The above integral can determine the burst pressure of thick-walled pipes if ε_1 and ε_2 are known at burst failure, but this integration is difficult to explicitly calculate because of its complexity. In order to calculate the integral in Eq. (23), the exponential generating function in the integrand can be expressed using the second (or even-index) Bernoulli numbers [49, 50], as shown in the following equation:

$$\frac{\frac{4\sqrt{3}}{2+\sqrt{3}}\varepsilon_A}{e^{\frac{4\sqrt{3}}{2+\sqrt{3}}\varepsilon_A}-1} = \sum_{k=0}^{\infty} \frac{B_k}{k!}\left(\frac{4\sqrt{3}}{2+\sqrt{3}}\varepsilon_A\right)^k \tag{24}$$

where B_k (k = 0, 1, 2, …, ∞) are the second Bernoulli numbers. The first ten nonzero second Bernoulli numbers have values: $B_0 = 1$, $B_1 = -\frac{1}{2}$, $B_2 = \frac{1}{6}$, $B_4 = -\frac{1}{30}$, $B_6 = \frac{1}{42}$, and $B_8 = -\frac{1}{30}$,

and $B_{10} = \frac{5}{66}$. The odd second Bernoulli numbers are zeros: $B_3 = B_5 = B_7 = B_9 = 0$. Using Eq. (24), calculation of the integral in Eq. (23) becomes an integration of a complex polynomial function that determines the following power series solution of the general applied pressure as:

$$P = \left(\frac{2+\sqrt{3}}{4\sqrt{3}}\right)^{n+1} \left(\frac{e}{n}\right)^{n} S_{uts} \sum_{k=0}^{\infty} \frac{B_k}{k!} \frac{\left(\frac{4\sqrt{3}}{2+\sqrt{3}}\varepsilon_1\right)^{k+n} - \left(\frac{4\sqrt{3}}{2+\sqrt{3}}\varepsilon_2\right)^{k+n}}{(k+n)} \tag{25}$$

Since ε_2 can be expressed as a function of ε_1, as evident from Eq. (A.8) in Appendix A, Equation (25) shows that the applied pressure P is a function of ε_1 only. From the P-ε_1 relation, the peak pressure can be determined. Alternatively, for a given value of n and κ, the burst strain ε_{1b} is solved from Eq. (A.10), and the burst strain ε_{2b} is calculated from Eq. (A.8). With the values of ε_{1b} and ε_{2b}, the exact solution of burst pressure can be determined from Eq. (23) by integration or directly calculated from the series solution in Eq. (25), but both exact solutions are not a closed-form.

3.4. Exact solution of burst pressure in a closed-form

This section investigates an exact solution of burst pressure in a closed-form that is fit well with the power series solution from Eq. (25) or the numerical integration result from Eq. (23).

For a strain non-hardening material (i.e., n = 0, or ideally plastic material), $K = S_{uts}$, and for a thick-walled pipe, integration of stress equilibrium Eq. (19) obtains the following closed-form exact solution of burst pressure in the closed-from for the Zhu-Leis yield criterion:

$$P_b = \frac{2+\sqrt{3}}{2\sqrt{3}} S_{uts} \ln\left(\frac{D_o}{D_i}\right) \tag{26}$$

For a thin-walled pipe with $D/t \geq 20$, Zhu et al. [51] showed that $\ln(D_o/D_i) \approx 2t/(D-t)$. In this case, Equation (26) reduces to the Zhu-Leis strength solution (i.e., Eq. (7) with n = 0) for the ideally plastic material.

For a power-law strain hardening material, Equation (26) suggests that the burst pressure solution of Eq. (23) or (25) for a thick-walled pipe may have the logarithmic function of $\ln(D_o/D_i)$ as its geometrical term and the same material parameter term of Eq. (7) as for a thin-walled pipe. Thus, the closed-form exact solution of burst pressure for a thick-walled pipe in the power-law strain hardening material is proposed to be expressed in the following closed-form for the Zhu-Leis yield criterion as:

$$P_b = 2\left(\frac{2+\sqrt{3}}{4\sqrt{3}}\right)^{n+1} S_{uts}\, ln\left(\frac{D_o}{D_i}\right) \tag{27}$$

Note that Zhu et al. [51] recently developed an modified strength theory and obtained a more accurate burst pressure solution as the same as Eq. (27) for a thick-walled pipe in a power-law strain hardening material. Johnson et al. [52] have validated the thick-wall burst pressure solution in Eq. (27) with FEA results for a wide range of pipeline sizes and grades.

3.5. General exact solutions of burst pressure for three yield criteria

Following the mathematical derivation of the Zhu-Leis flow solution in Eq. (25) or (27) for thick-walled pipes, the flow solutions of burst pressure are also obtained for the Tresca and von Mises yield criteria, respectively, where the Tresca effective stress in Eq. (14a) and Tresca effective strain in Eq. (14b) as well as the von Mises effective stress in Eq. (15a) and von Mises effective strain in Eq. (15b) are used. As a result, using the second Bernoulli numbers, a general power series solution of burst pressure for thick-walled pipes is obtained in terms of the Tresca, von Mises and Zhu-Leis yield criteria as follows:

$$P_b = \left(\frac{C}{2}\right)^{n+1} \left(\frac{e}{n}\right)^n S_{uts} \sum_{k=0}^{\infty} \frac{B_k}{k!} \frac{\left(\frac{2}{C}\varepsilon_{1b}\right)^{k+n} - \left(\frac{2}{C}\varepsilon_{2b}\right)^{k+n}}{(k+n)} \tag{28}$$

where C is a constant that is related to the yield criterion and defined as:

$$C = \begin{cases} 1, & \text{for Tresca yield criterion} \\ \frac{2}{\sqrt{3}}, & \text{for von Mises yield criterion} \\ \frac{1}{2} + \frac{1}{\sqrt{3}}, & \text{for Zhu-Leis yield criterion} \end{cases} \tag{29}$$

At the burst failure of the thick-walled pipe, the burst strains ε_{1b} and ε_{2b} in Eq. (28) are determined from Eqs. (A.8) and (A.10) that are given in Appendix A.

Alternatively, as similar to Eq. (27), the general exact solution of burst pressure for thick-walled pipes can be expressed in the following closed-form function for the Tresca, von Mises, or Zhu-Leis yield criterion:

$$P_b = 2\left(\frac{C}{2}\right)^{n+1} S_{uts}\, ln\left(\frac{D_o}{D_i}\right) \tag{30}$$

The closed-form exact solution of burst pressure in Eq. (30) for thick-walled pipes is the same as that given by Zhu et al. [51] from a new modified strength theory. The next section will verify that the closed-form exact solution in Eq. (30) is equivalent to the power series solution in Eq. (28) for each yield criterion for a wide range of n and κ values.

3.6. Analyses and results of burst strain, burst stress and burst pressure

This section presents the analyses and results of the Zhu-Leis exact solutions of the burst strains, burst stresses and burst pressure for thick-walled pipes, where the burst effective strains are obtained from Eqs. (A.8) and (A.10), the burst effective stresses are obtained from Eq. (9), and the burst pressure is obtained by integrating Eq. (23) or directly calculated from the power series solution in Eq. (25) (using the first ten terms) for different values of $\kappa = D_o / D_i$ and n in terms of the Zhu-Leis criterion. The power series solution of burst pressure is then compared with the closed-from exact solution in Eq. (27) for the Zhu-Leis criterion to verify the validity of this closed-form exact solution.

Figures 2 and 3 show the variations of Zhu-Leis burst strains ε_{1b} and ε_{2b} and Zhu-Leis burst stresses σ_{1b} and σ_{2b} with the diameter ratio of D_o / D_i , respectively, for five given strain hardening exponent values of n = 0.05, 0.10, 0.15, 0.20, and 0.25. Figure 2 shows that 1) the two Zhu-Leis burst strains are nonlinearly related to D_o / D_i, 2) all ε_{1b} values are larger than the corresponding ε_{2b} values for a given n, and 3) all ε_{1b} values increase, but the ε_{2b} values decrease as D_o / D_i increases for a given n. Figure 3 shows that 1) the two Zhu-Leis burst stresses are also nonlinearly related to D_o / D_i, 2) the Zhu-Leis burst stress σ_{1b} normalized by the true UTS increases with D_o / D_i for a given n, and 3) the normalized Zhu-Leis burst stress σ_{2b} decreases as both D_o / D_i and n increase.

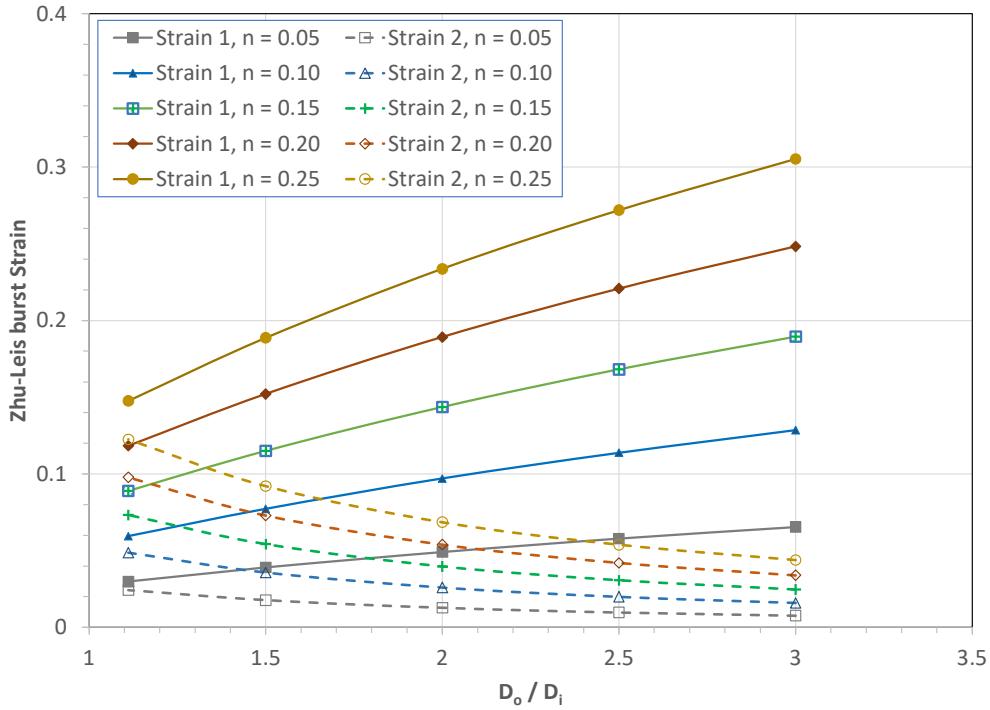

Figure 2. Variation of Zhu-Leis strain at burst failure with D_o / D_i for five given n values.

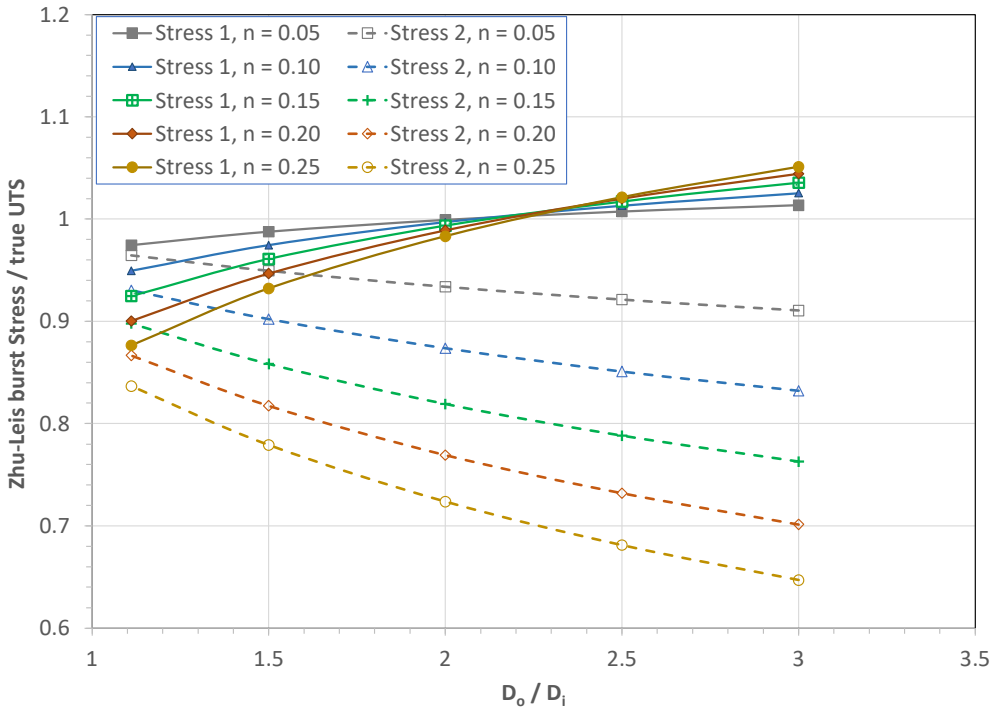

Figure 3. Variation of Zhu-Leis stress at burst failure with D_o / D_i for five n values.

Using the above determined values for Zhu-Leis burst strains ε_{1b} and ε_{2b}, the Zhu-Leis burst pressure is calculated directly from the power series solution in Eq. (25) with the first ten terms (or by integrating Eq. (23) with the trapezoidal rule and 50 equal incremental steps of integration). Figure 4 depicts variations of the Zhu-Leis burst pressure ratio, $\frac{P_b}{S_{uts}}$, with the geometrical term $\ln\left(\frac{D_o}{D_i}\right)$ calculated from Eq. (25) for five given values of n = 0.05, 0.10, 0.15, 0.20, and 0.25. Also included in Fig. 4 for comparison is the closed-form exact Zhu-Leis flow solution of burst pressure in Eq. (27). The comparison shows that the proposed Zhu-Leis flow solution in Eq. (27) agrees well with the calculated data for all n values (note that the power series solution is slightly lower than the closed-form exact solution for larger values of D_o / D_i and n. This is likely caused by the ten-term selection in Eq. (28)). From this observation, it can be concluded that the proposed Zhu-Leis flow solution in Eq. (27) is a closed-form exact solution of burst pressure for thick-walled pipes when the Zhu-Leis yield criterion is adopted.

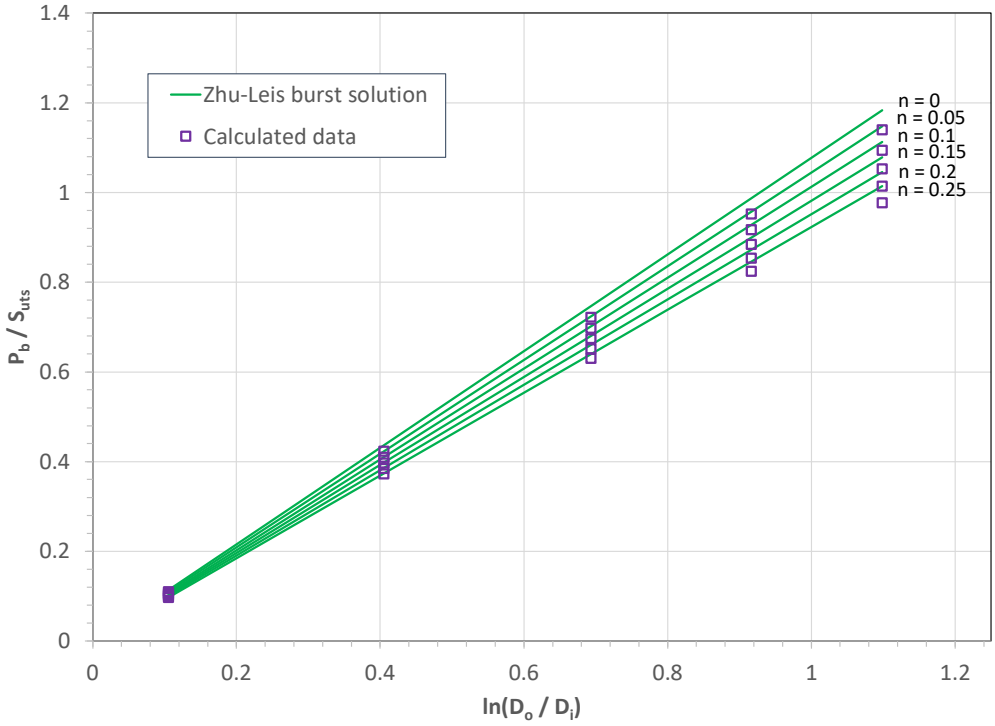

Figure 4. Zhu-Leis burst pressure ratio $\frac{P_b}{S_{uts}}$ against $\ln\left(\frac{D_o}{D_i}\right)$ for five given n values.

In the similar manner, the von Mises exact solutions of burst strains, burst stresses and burst pressure for thick-walled pipes are obtained and given in Appendix B, and the Tresca exact solutions of burst strains, burst stresses and burst pressure for thick-walled pipes are obtained and given in Appendix C.

Figure 5 compares three burst pressure predictions by the von Mises, Zhu-Leis and Tresca yield criteria with the strain hardening exponent, n, for thick-walled pipes, where the predicted pressures are normalized by the Tresca strength solution, $P_b = S_{uts} \ln(D_o/D_i)$. Also included in this figure are three power series solutions from Eq. (28) with use of the first ten terms and the numerical results from a new FEA burst model that was recently obtained by Johnson et al. [52]. From Fig. 5, the following observations are made:

1) The von Mises exact solution agrees well with the von Mises power series solution, and both provides an upper bound prediction of burst pressure for thick-walled pipes,
2) The Tresca exact solution agrees well with the Tresca power series solution, and both provides a lower bound prediction of burst pressure for thick-walled pipes,
3) The Zhu-Leis exact solution agrees well with the Zhu-Leis power series solution, and both provides an intermediate prediction of burst pressure for thick-walled pipes, and
4) The Zhu-Leis exact solution matches well with the FEA results, which confirms that the Zhu-Leis exact solution is an accurate prediction of burst pressure for thick-walled pipes.

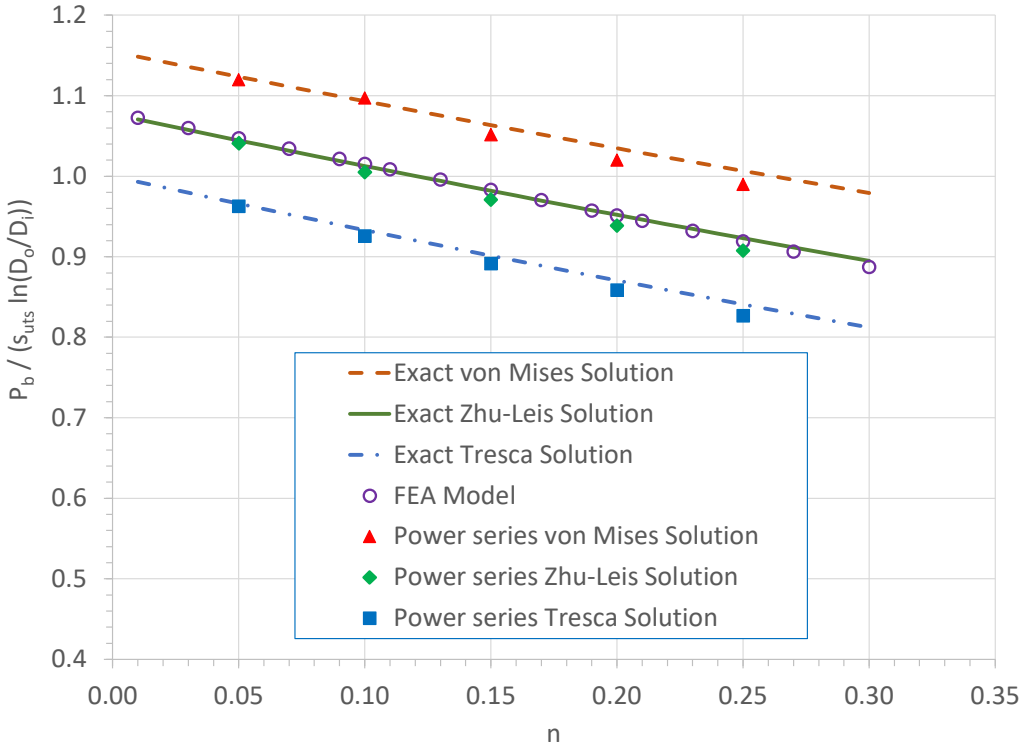

Figure 5. Comparison of normalized burst pressures varied with n for three yield criteria

4. Experimental validation

This section assesses the four existing burst pressure models in Eqs. (1) to (4) and the proposed exact solutions of burst pressure in Eq. (30) from the flow theory of plasticity in terms of the von Mises, Tresca and Zhu-Leis criteria for thick-walled pipes. Two datasets of burst pressure tests are utilized here to evaluate these burst prediction models for thick-walled pipes with capped ends. One dataset contains burst test data for small diameter, thick-walled tubes, and the other dataset contains burst test data for large diameter, thin and thick-walled pipes.

4.1 Validation with burst test data for thick-walled tubes

In the early 1950s, Faupel [37-38] conducted about one hundred burst pressure tests over a period of seven years and obtained the burst test data for small diameter, thick-walled pressure tubes in various metals, including plain carbon steels, stainless steels, gun steels, low alloy steels, weld steels, aluminum, and bronze. The test tubes were very thick, leading to a small D/t ratio in the range of $2.4 < D/t < 4.7$. From these burst tests, thirty burst test data for plain carbon steels designated as AISI 1025, AISI 1030, AISI 3130, AISI 3320, AISI 4130, AISI 4140, and AISI 4340 are selected and used in this work for evaluating the burst prediction models for thick-

walled tubes. The materials for these burst tests were low, medium, or high carbon steels with the yield strength in the range of 244 to 1076 MPa and the tensile strength in the range of 459 to 1119 MPa. The strain hardening exponent n of these tube steels is less than 0.25. Note that the burst test data obtained by Faupel [37] were also reported by Christopher et al. [11] in their Table 5.

Figure 6 compares the burst pressure predictions with measured burst pressure data that were obtained by Faupel [37] for small diameter, thick-walled pressure tubes, where the y-axis represents the burst pressure normalized by the Tresca strength solution, $P_b = S_{uts} \ln\left(\frac{D_o}{D_i}\right)$, for thick-walled pipes, and the x-axis denotes the material strain hardening exponent n. The burst pressure predictions were determined from the four representative models for thick-walled pipes: the Turner model (i.e., Tresca strength solution) in Eq. (1), the Nadai model (i.e., von Mises strength solution) in Eq. (2), the Faupel empirical model in Eq. (3), the Svensson approximate model in Eq. (4), and the three proposed exact flow solutions in Eq. (30), including the von Mises flow solution, Tresca flow solution and Zhu-Leis flow solution.

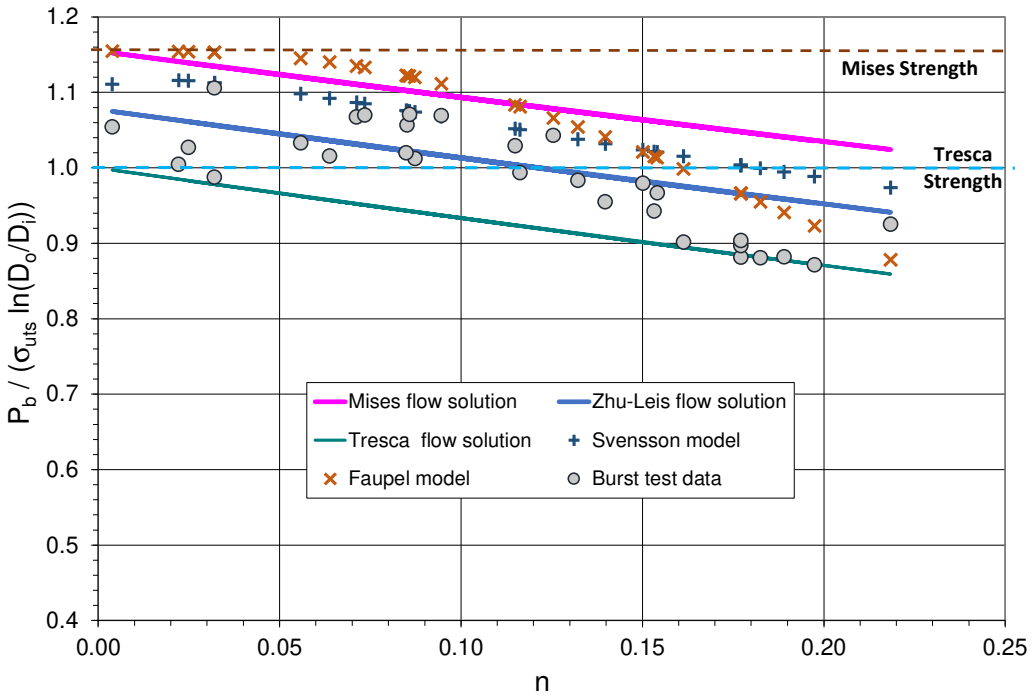

Figure 6. Comparison of exact burst pressure predictions with burst test data for thick-walled tubes as a function of n.

From Fig. 6, the following observations are determined:

1) The von Mises strength solution is independent of n, and provides an absolute upper bound prediction of the burst data.
2) The Tresca strength solution is independent of n, but provides an adequate burst pressure prediction, particularly for n < 0.1.

3) The von Mises flow solution is an upper bound prediction of the burst data for all n values.
4) The Tresca flow solution is a lower bound prediction of the burst data for all n values.
5) The Faupel empirical model provides comparable results to the Mises strength solution for low hardening strain materials with $n < 0.06$, and then its prediction decreases with n in a nearly linear trend. For most ductile steels with $n < 0.15$, the Faupel solution varies around the von Mises flow solution, and thus it overestimates the burst data. For high strain hardening steels with $0.15 < n < 0.22$, the Faupel solution seems to give an acceptable prediction of the burst data.
6) The approximate Svensson model predicts outcomes that are smaller than and nearly parallel to the Mises flow solutions for all n values. However, this Svensson model overestimates most of the burst data.
7) The Zhu-Leis flow solution is an intermediate prediction and agrees well with the burst data for all n values on average. Thus, this solution is the best prediction model.

Figure 7 illustrates the statistical analysis results of the burst pressure prediction to test data ratios (i.e., the burst pressure predictions normalized by the burst test data shown in Fig. 6) for the small diameter, thick-walled tubes, where the burst pressure is predicted by the von Mises strength model (or Nadai model), Tresca strength model (or Turner model), von Mises flow solution, Tresca flow solution, Zhu-Leis flow solution, Svensson model, and Faupel model. In particular, Fig. 7(a) shows the mean errors of these prediction models, and Fig. 7(b) shows the standard errors of these prediction models. Note that the standard error of the mean is a measure of how far each observed value from the mean of a dataset, and the mean error is an averaged measure of the relative errors between a model prediction and the corresponding test data for all data points in a dataset. A positive mean error denotes that a model overestimates test data, and a negative mean error denotes that a model underestimates test data. Accordingly, it follows from this figure that:

1) The von Mises strength solution has the largest mean error and the largest standard error,
2) The Tresca strength solution has the smallest mean error but a second large standard error,
3) The von Mises flow solution has a second large mean error and a third large standard error,
4) The Tresca flow solution has a large negative mean error and a small standard error,
5) The Zhu-Leis flow solution has a small mean error and a small standard error, and
6) The Svensson and Faupel models have a similar large mean error and a similar small standard error.

The statistical theory determines that the smaller the mean error and the standard error are, the more accurate a prediction model will be for the same set of experimental data. Thus, the results of statistical error analysis in Fig. 7 confirm the observations made in Fig. 6, that is, *the*

Zhu-Leis flow solution is the best prediction model of burst pressure, while the Svensson and Faupel models significantly overestimate the burst pressure for thick-walled pipes.

(a)

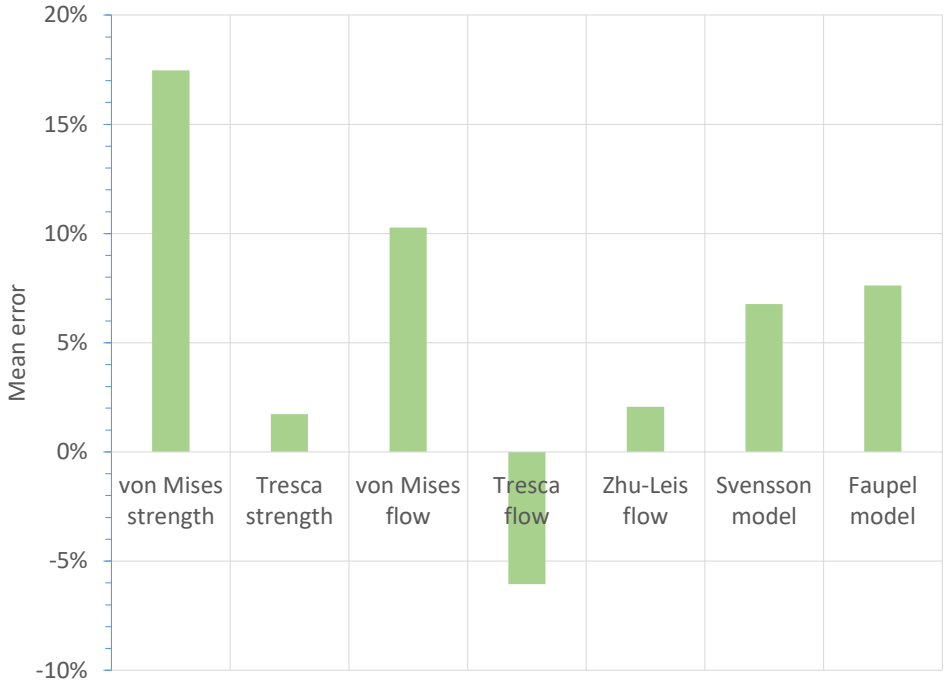

(b)

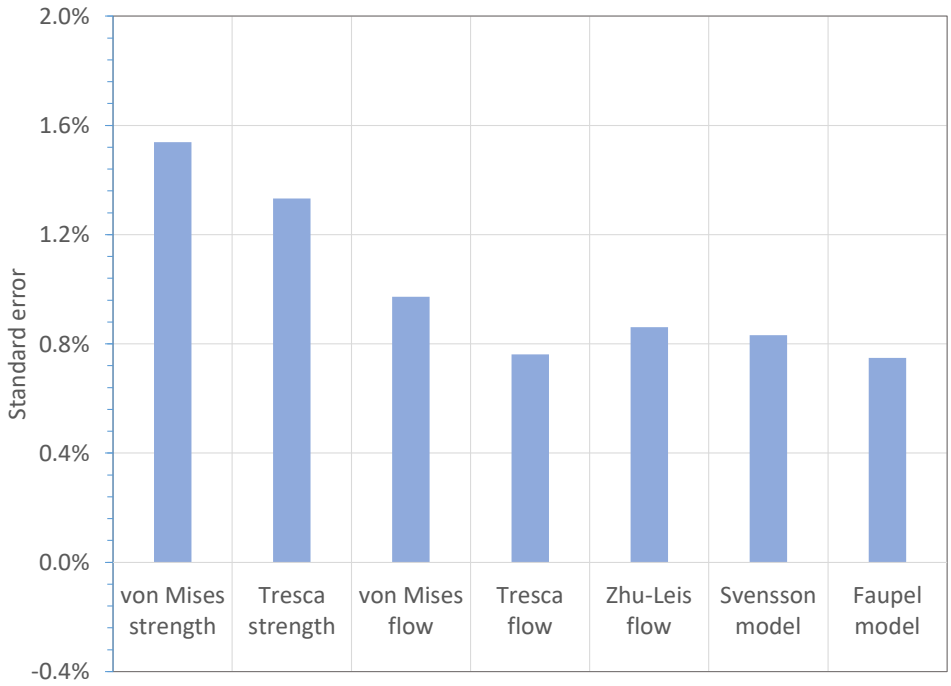

Figure 7. Statistical analysis results of the burst pressure prediction to test data ratio: (a) mean error, and (b) standard error.

From the above model evaluations, it is concluded that for thick-walled pipes that 1) the Nadai (i.e., von Mises strength solution), Faupel, and Svensson models all overpredict the burst data, 2) the Turner model (i.e., Tresca strength solution) overall determines adequate predictions of all burst data, 3) the Mises flow solution is an upper bound prediction, 4) the Tresca flow solution is a lower bound solution, and 5) the Zhu-Leis flow solution is an intermediate solution that predicts the best results compared to the burst data on average.

4.2 Validation with burst test data for thin and thick-walled pipes

In 2007, Zimmermann et al. [28] collected 37 burst test data for large diameter, thin and thick-walled pipes that were obtained by the European Pipeline Research Group (EPRG) for evaluating a set of burst prediction models. The pipe materials are either pipeline steels or structural carbon steels, and the diameter to thickness ratio varies in the range of $10 < D/t < 80$. The pipe steels have the yield strengths in the range of 264 to 807 MPa and the tensile strengths in the range of 392 to 869 MPa. The strain hardening exponents n of the pipe steels are all less than 0.20.

Figure 8 compares the burst pressure predictions with measured burst data that were given by Zimmermann et al. [17] for large diameter, thin and thick-walled pipes, where the y-axis represents the burst pressure normalized by the Tresca strength solution, $P_b = S_{uts} \ln\left(\frac{D_o}{D_i}\right)$, for thick-walled pipes, and the x-axis denotes the strain hardening exponent n. The burst pressure predictions were obtained from the four representative models for thick-walled pipes: the Turner model (i.e., Tresca strength solution) in Eq. (1), the Nadai model (i.e., von Mises strength solution) in Eq. (2), the Faupel empirical solution in Eq. (3), the Svensson approximate solution

in Eq. (4), and the three proposed flow solutions including the von Mises flow solution, Tresca flow solution and Zhu-Leis flow solution in Eq. (30).

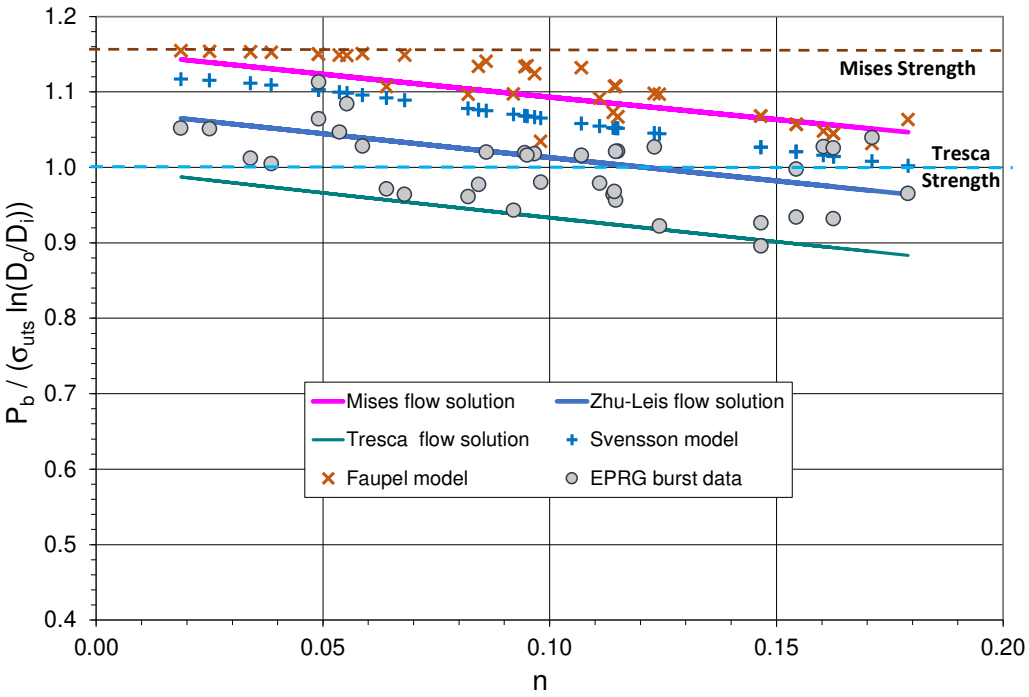

Figure 8. Comparison of burst pressure predictions with burst test data for thin and thick-walled pipes as a function of n.

Comparison of Fig. 8 with Fig. 6 shows all prediction results in these two figures are similar, and thus all observations obtained in Fig. 6 are also applicable to Fig. 8 for the EPRG burst data.

Figure 9 plots the statistical analysis results of the burst pressure prediction to test data ratios (i.e., the burst pressure predictions normalized by the burst test data shown in Fig. 8) for the large diameter, thin and thick-walled pipes, where the burst pressure is predicted by the von Mises strength model (or Nadai model), Tresca model (or Turner model), von Mises flow solution, Tresca flow solution, Zhu-Leis flow solution, Svensson model, and Faupel model. In particular, Fig. 9(a) shows the mean errors of these prediction models, and Fig. 9(b) shows the standard errors of these prediction models. Comparison of Fig. 9 with Fig. 7 shows that all statistical errors are similar for each prediction model, and thus all observations made in Fig. 7 are applicable to Fig. 9 for the EPRG burst data. As a result, it is again concluded that *the Zhu-Leis flow solution is the best prediction model of burst pressure, while the Svensson and Faupel models significantly overestimate burst pressure for thick-walled pipes*.

(a)

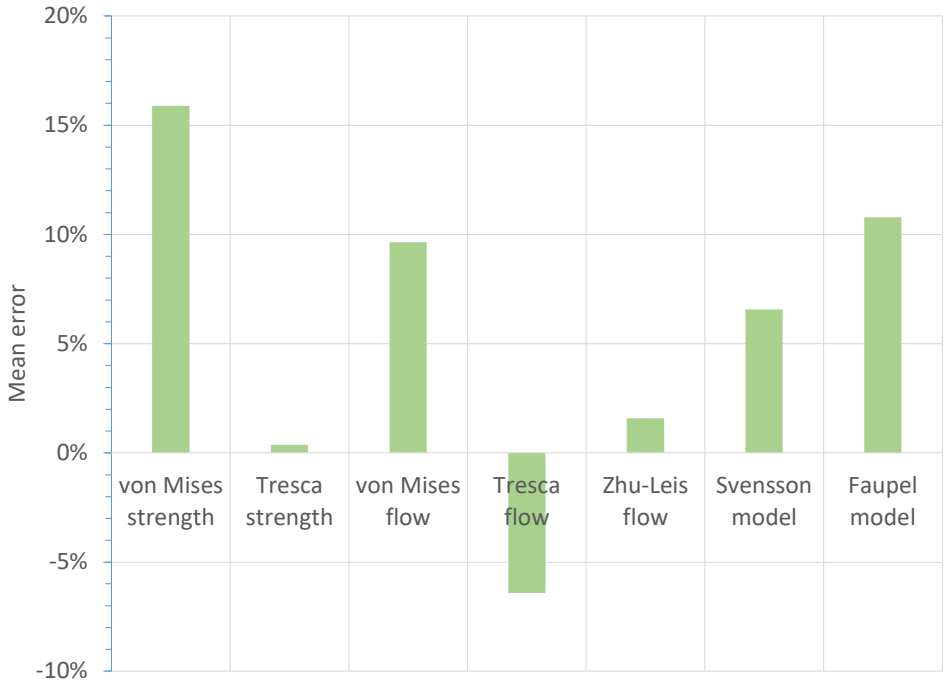
20%
15%
10%
5%
0%
-5%
-10%
Mean error
von Mises strength
Tresca strength
von Mises flow
Tresca flow
Zhu-Leis flow
Svensson model
Faupel model

(b)

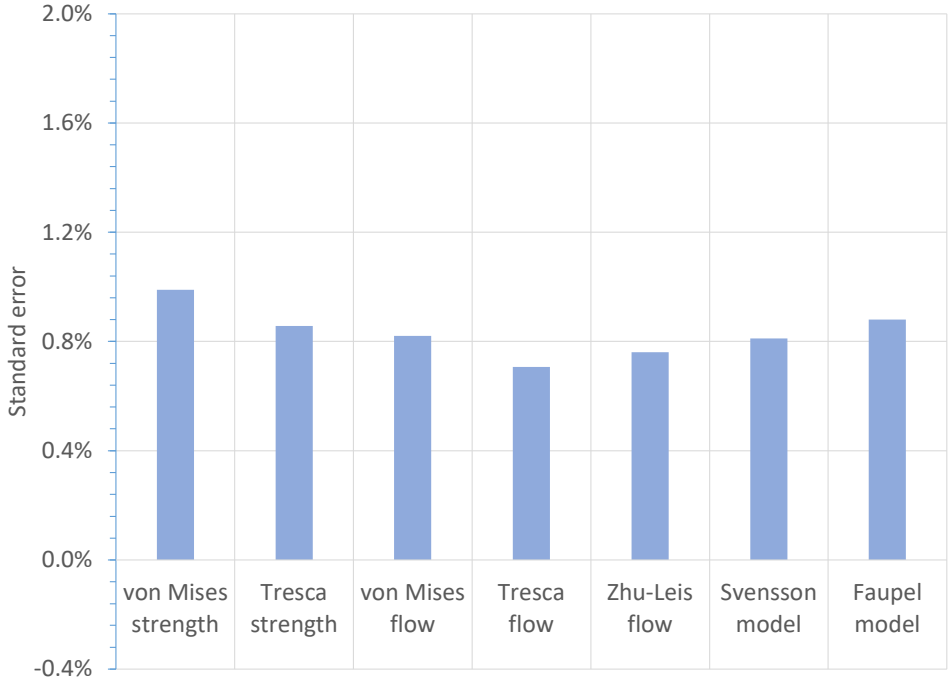
2.0%
1.6%
1.2%
0.8%
0.4%
0.0%
-0.4%
Standard error
von Mises strength
Tresca strength
von Mises flow
Tresca flow
Zhu-Leis flow
Svensson model
Faupel model

Figure 9. Statistical analysis results of the burst prediction to test data ratio: (a) mean error, and (b) standard error.

In summary, the experimental evaluations performed above validate that the Zhu-Leis flow solution for thick-wall pipes can accurately predict burst pressure for both thin and thick-walled pipes with small to large D/t ratios. In contrast, the Mises and Tresca flow solutions can serve as the upper and lower bound predictions of burst pressure for the thick-walled pipes.

5. Conclusions

This paper developed three exact solutions of burst pressure for defect-free, thick-walled pipes with capped ends using the flow theory of plasticity in terms of the Tresca, von Mises, and Zhu-Leis yield criteria, respectively. It was assumed that the pipe steel obeys the power-law strain hardening rule, and the large plastic deformation was described by the finite strain theory. On this basis, internal pressure was determined as a power series function of the effective strains on the inside and outside surfaces of the thick-walled pipe with use of the second Bernoulli numbers. At burst failure, these effective strains and stresses were obtained, and then three flow solutions of burst pressure were determined as a power series solution in a function of the D_o/D_i ratio, n, and UTS. In order to determine a closed-form exact solution, a general flow solution of burst pressure was then proposed for the three yield criteria, and the results showed that the proposed exact solution matches well with the power series solution for each yield criterion. Two datasets of full-scale burst tests were then utilized to evaluate the four existing burst prediction models and the three proposed flow solutions of burst pressure for thick-walled pipes. The final results are concluded as follows:

1) The Nadai model (i.e., von Mises strength solution), the empirical Faupel model, and the approximate Svensson model all significantly overpredict the burst pressure, and thus their burst pressure predictions are nonconservative.
2) The Turner model (i.e., Tresca strength solution) overall determines an adequate prediction of the burst pressure data, particularly for $n < 0.1$, and thus its predictions may be acceptable for engineering applications.
3) The von Mises power series solution is equivalent to the von Mises flow solution, and serves as an upper bound prediction of burst pressure for both thin and thick-walled pipes.
4) The Tresca power series solutions is equivalent to the Tresca flow solution, and serves as a lower bound solution of burst pressure for both thin and thick-walled pipes.
5) The Zhu-Leis power series solution is equivalent to the Zhu-Leis flow solution, and serves as an intermediate prediction that correlates best with burst pressure data on average.
6) The Zhu-Leis flow solution agrees well with the FEA burst model results obtained recently by Johnson et a. [52] for thick-walled pipes.

In summary, the Zhu-Leis flow solution is an accurate closed-form exact solution of burst pressure for thin and thick-walled pipes. This exact solution of burst pressure is limited to applications for power-law strain hardening materials, including ductile steels and ductile polymers, but may be not applicable to brittle metals or other non-power-law strain hardening materials. In practical applications, the thin-wall based Zhu-Leis flow solution in Eq. (7) is recommended predict burst pressure for thin-walled pipes or cylinders with a large D/t ratio of $D/t > 20$, whereas the thick-wall based Zhu-Leis flow solution in Eq. (27) is recommended predict burst pressure for thick-walled pipes or tubes with a small D/t ratio of $D/t \leq 10$. See Reference [51] for more discussions on when to use an appropriate flow solution to predict burst pressure for pressure pipes with a different D/t ratio. In addition, Further experimental validations are recommended for ensuring the general validity of the proposed exact solutions of burst pressure for various thick-walled pipes with different geometries or different materials.

Acknowledgements

This work was financially supported by the Laboratory Directed Research and Development (LDRD) program within the Savannah River National Laboratory (SRNL). This document was prepared in conjunction with work accomplished under Contract No. 89303321CEM000080 with the U.S. Department of Energy (DOE) Office of Environmental Management (EM).

References

[1] Transportation Research Board, *Transmission Pipelines and Land Use*, Special Report 281, Washington, D.C., 2004.
[2] Wang L, Zhang Y. Plastic collapse analysis of thin-walled pipes based on unified yield criterion, *International Journal of Mechanical Sciences*, Vol. 53(5), 2011: 348-354.
[3] Lyons CJ, Race JM, Change E., Cosham A, Wetenhall B, Barnett J. Validation of the NG-18 equations for thick-walled pipelines, *Engineering Failure Analysis*, Vol. 112, 2020: 104494.
[4] Hamada M, Yokoyama R, Kitagawa H. An estimation of maximum pressure for a thick-walled tube subjected to internal pressure, *International Journal of Pressure Vessels and Piping*, 22, 1986: 311-323.
[5] Kadam M, Balamurugan G, Bujurke AA, Joshi KM. Finite element prediction of static burst pressure in closed thick-walled unflawed cylinders of different diameter ratios, *Procedia Engineering*, Vol. 173, 2017: 577-594.
[6] Barashkov VN, Shevchenko MY. Elastic-plastic stress-strain state and strength of thick-walled pipe under the action of internal pressure, *Journal of Physics*, Vol. 1214, 2019: 012008.
[7] Wang H, Zheng T, Sang Z, Krakauer BW. Burst pressures of thin-walled cylinders constructed of steel exhibiting a yield plateau, *International Journal of Pressure Vessels and Piping*, Vol. 193, 2021: 104483.
[8] Zhu XK. A comparative study of burst failure models for assessing remaining strength of corroded pipelines, *Journal of Pipeline Science and Engineering*, Vol. 1(1), 2021: 36-50.
[9] Sun M, Chen Y, Zhao H, Li X. Analysis of the impact factor of burst capacity models for defect-free pipelines, *International Journal of Pressure Vessels and Piping*, Vol. 200, 2022: 104805.
[10] Zhu XK. Recent advances in corrosion assessment models for buried transmission pipelines, *Journal of CivilEng*, Vol. 4(2), 2023: 391-415.
[11] Christopher T, Rama Sarma BS, Govinda Potti PK, Rao BN. A comparative study on failure pressure estimation of unflawed cylindrical vessels, *International Journal of Pressure Vessels and Piping*, Vol. 79, 2002: 53-66.
[12] Krishnaveni A, Christopher T, Jeyakumar K, Jebakani D. Probabilistic failure prediction of high strength steel rocket motor cases, *Journal of Failure Analysis and Prevention*, Vol. 14, 2014: 478-490.
[13] Zhu XK, Leis BN, Evaluation of burst pressure prediction models for line pipes, *International Journal of Pressure Vessels and Piping*, Vol. 89, 2012: 85-97.
[14] Law M, Bowie G, Prediction of failure strain and burst pressure in high yield to-tensile strength ratio linepipe, *International Journal of Pressure Vessels Piping*, Vol. 84, 2007: 487-492.

[15] Zhu XK, Strength criteria versus plastic flow criteria used in pressure vessel design and analysis, *Journal of Pressure Vessel Technology*, Vol. 138, 2016: 041402.
[16] Oh, DH, Race J, Oterkus S, Chang E. A new methodology for the prediction of burst pressure for API 5L X grade flawless pipelines, *Ocean Engineering*, Vol. 212, 2020: 107602.
[17] Engineering ToolBox. *Barlow's Formula – Internal, Allowable and Bursting Pressure*, 2005. Online Available at www.engineeringtoolbox.com/barlow-d_1003.html.
[18] ASME BPVC-2021, *Boiler and Pressure Vessel Code*, American Society of Mechanical Engineers, New York.
[19] ASME B31.3-2020, *Pressure Design of Straight Pipe for Internal Pressure*, American Society of Mechanical Engineers, New York.
[20] Cooper WE. The significance of the tensile test to pressure vessel design, *Welding Journal - Welding Research Supplement*; January 1957: 49s-56s.
[21] Svensson N.L. The bursting pressure of cylindrical and spherical vessels, *Journal of Applied Mechanics,* Vol. 25, 1958: 89-96.
[22] Weil NA. Tensile instability of thin-walled cylinders of finite length, *International Journal of Mechanical Sciences*, Vol. 5(6), 1963: 487-506.
[23] Hillier MJ. Tensile plastic instability of thin tubes-I, *Internal Journal of Mechanical Sciences*, Vol. 7(8), 1965: 531-538.
[24] Kiefner JF, Macey WA, Duffy AR. *The significance of the yield-to-ultimate strength ratio of line pipe materials*, Summary Report to Pipeline Research Committee, American Gas Association, March 2971.
[25] Stewart G, Klever FJ. An analytical model to predict the burst capacity of pipelines, *Proceedings of International Conference of Offshore Mechanics and Arctic Engineering*. Vol. V, Pipeline Technology, 1994: 177-188.
[26] Zhu XK, Leis BN. Accurate prediction of burst pressure for line pipes, *Journal of Pipeline Integrity*, Vol. 4, 2004: 195-206.
[27] Zhu XK, Leis BN. Average shear stress yield criterion and its application to plastic collapse analysis of pipelines, *International Journal of Pressure Vessels and Piping*, Vol. 83, 2006: 663-671.
[28] Zimmermann S, Hohler S, Marewski U. Modeling ultimate limit states on burst pressure and yielding of flawless pipes, *Proceedings of the 16th Biennial Pipeline Research Joint Technical Meeting*, Canberra, Australia, April 16-19, 2007. Paper 13.
[29] Knoop FM, Flaxa V, Zimmermann S, Grob-Weege J. Mechanical properties and component behavior of x80 helical seam welded large diameter pipes, *Proceedings of the 8th International Pipeline Conference*. Calgary, Alberta, Canada; September 27-October 1, 2010.
[30] Bony M, Alamilla JL, Vai R, Flores E. Failure pressure in corroded pipelines based on equivalent solutions for undamaged pipe, *Journal of Pressure Vessel Technology*, Vol. 132, 2010: 051001.
[31] Zhou W, Huang G, Model error assessment of burst capacity models for defect-free pipes, *Proceedings of the 9th International Pipeline Conference*, Calgary, Canada, September 24-28, 2012.
[32] Wang Q, Zhou W. Burst pressure models for thin-walled pipe elbows, *International Journal of Mechanical Sciences*, Vol. 159, 2019: 20-29.

[33] Chen Z, Li X, Wang W, et al. Dynamic burst pressure analysis of cylindrical shells based on average shear stress yield criterion, *Thin-Walled Structures*, Vol. 148, 2020: 106498.
[34] Yang J, Hu S. Estimation of burst pressure of PVC pipe using average shear stress yield criterion: Experimental and numerical studies, *Applied Science*, Vol. 11 (21), 2021: 10477.
[35] Deng K, Lin Y, Li B, Wang X. Investigation on the calculation model of burst pressure for tube and casing under practical service environment, *International Journal of Hydrogen Energy*, Vol. 44, 2019: 23277-23288.
[36] Deng K, Peng Y, Liu B, Lin Y, Wang J. Through-wall yield ductile burst pressure of high-grade steel tube and casing with and without corroded defect, *Marine Structures*, Vol. 76, 2021: 102902.
[37] Faupel JH. Yield and bursting characteristics of heavy-wall cylinders, Transaction of ASME, *Journal of Fluid Engineering*, Vol. 78 (5), 1956: 1031-1064.
[38] Faupel JH, Furbeck AR. Influence of residual stress on behavior of thick-wall closed-end cylinders, Transactions of ASME, *Journal of Fluid Engineering*, Vol. 75(4), 1953: 345-354.
[39] Harvey JF. *Theory and Design of Pressure Vessels*, Van Nostrand Reinhold, New York, USA, 1991.
[40] Hamgung I, Giang NH. Investigation of burst pressures in PWR primary pressure boundary components, *Nuclear Engineering and Technology*, Vol. 48, 2016: 236-245.
[41] Kang SG, Young KJ. Modified Svensson's formula for more accurate burst pressure predictions of thin cylindrical shells with small length to diameter ratios, *Proceedings of the ASME 2015 Pressure Vessels and Piping Conference*, July 19-23, 2015, Boston, MA, USA.
[42] Mohan A, Jaisingh SJ, Priscilla CPG. Effect of autofrettage on the ultimate behavior of thick cylindrical pressure vessels, *International Journal of Pressure Vessels and Piping*, Vol. 194, 2021: 104546.
[43] Crossland, J.A. Bones, Behavior of thick-walled steel cylinders subjected to internal pressure, *Proceeding of the Institution of Mechanical Engineers*, Vol. 172 (1), 1958: 777-804.
[44] Martin J, Weng TL. Strength of thick-walled cylindrical pressure vessels, *Journal of Engineering Industry*, Vol. 85, 1963: 405-416.
[45] Turner LB. The stresses in a thick hollow cylinder subjected to internal pressure, *Transactions of Cambridge Philosophical Society*, Vol. 21, 1910: 377-396.
[46] Nadai A. *Plasticity*, McGra-Hill, New York, 1931.
[47] Zhu XK, Leis BN. Influence of yield-to-tensile strength ratio on failure assessment of corroded pipelines, *Journal of Pressure Vessel Technology*, Vol. 127, 2005: 436-442.
[48] MacGregor C.W., Coffin L.F., Fisher J.C., The plastic flow of thick-walled tubes with large strains, *Journal of Applied Physics*, Vol. 19, 1948: 29-297.
[49] Arfken GB and Weber, HJ. Bernoulli numbers, Euler-Maclaurin formula, in *Mathematical Methods for Physicists*, 4th edition, Academic Press, San Diego, California, 1995, pp. 338-348.
[50] Larson ND, *The Bernoulli Numbers: A Brief Primer*, A Master Thesis, Whitman College, WA, USA, May 10, 2019.
[51] XK Zhu, Wiersma B, Johnson WR, Sindelar R. Burst pressure solutions of thin and thick-walled cylindrical vessels, *Journal of Pressure Vessel Technology*, Vol. 145, 2023: 044202.
[52] Johnson WR, Zhu XK, Sindelar R, Wiersma B. A parametric finite element study for determining burst strength of thin and thick-walled pressure vessels, *International Journal of Pressure Vessels and Piping*, Vol. 204, 2023: 104968.

Appendix A. Burst Strains for Thick-Walled Pipes

A.1 Burst failure conditions

Equation (23) shows that the applied pressure *P* can be a function of the effective strains ε_1 in the case where ε_2 is a function of ε_1. The burst pressure P_b is then determined at the plastic instability condition, that is, the differential of *P* with regard to ε_1 is equal to zero:

$$\frac{\partial P}{\partial \varepsilon_1} = \frac{\varepsilon_2^n}{1-e^{\frac{2}{C}\varepsilon_2}} \frac{\partial \varepsilon_2}{\partial \varepsilon_1} - \frac{\varepsilon_1^n}{1-e^{\frac{2}{C}\varepsilon_1}} = 0 \tag{A.1}$$

where $C = \frac{2+\sqrt{3}}{2\sqrt{3}}$ for the Zhu-Leis yield criterion or see Eq. (29) for other yield criteria. The above equation leads to a relationship between the two burst strains ε_{1b} and ε_{2b} at the plastic instability of the thick-walled pipe:

$$\left(\frac{\varepsilon_{1b}}{\varepsilon_{2b}}\right)^n = \frac{1-e^{\frac{2}{C}\varepsilon_{1b}}}{1-e^{\frac{2}{C}\varepsilon_{2b}}} \left.\frac{\partial \varepsilon_2}{\partial \varepsilon_1}\right|_b \tag{A.2}$$

where all variables with the subscription *b* denotes the variables at the pipe burst condition.

A.2 Relation between ε_1 and ε_2

From Eq. (20), the strain compatibility equation for the Zhu-Leis yield criterion is rewritten as:

$$\frac{d\varepsilon_A}{1-e^{\frac{2}{C}\varepsilon_A}} = \frac{C}{x} dx \tag{A.3}$$

where $x = \frac{(r+u)}{R_i}$ is a normalized current radius of the point in consideration. On the ID surface, the hoop strain $\varepsilon_{\theta\theta} = ln(x_1)$, and thus the effective stress ε_1 is given by:

$$\varepsilon_1 = \frac{C}{2} \ln(x_1^2) \tag{A.4}$$

With the strain boundary condition in Eq. (A.4), integrating Eq. (A.3) obtains:

$$\varepsilon_A = \frac{C}{2} \ln\left(\frac{x^2}{1-x_1^2+x^2}\right) \tag{A.5}$$

Because plastic deformation is incompressible, the volume of the pipe remains unchanged during the plastic deformation, and thus the following geometrical relationship is obtained:

$$x_2^2 - x_1^2 + 1 = \kappa^2 \tag{A.6}$$

where $\kappa = D_o/D_i$ is the diameter ratio of the pipe. From Eqs. (A.5) and (A.6), the effective strain ε_2 on the OD surface is obtained:

$$\varepsilon_2 = \frac{C}{2}\ln\left(\frac{\kappa^2-1+x_1^2}{\kappa^2}\right) \tag{A.7}$$

From Eqs. (A.4) and (A.7), after eliminating x_1, the effective strain ε_2 is related to ε_1 in the form:

$$\varepsilon_2 = \frac{C}{2}\ln\left(1-\frac{1-e^{\frac{2}{C}\varepsilon_1}}{\kappa^2}\right) \tag{A.8}$$

From this equation, the differential of ε_2 with regard to ε_1 is obtained as:

$$\frac{\partial\varepsilon_2}{\partial\varepsilon_1} = \frac{e^{\frac{2}{C}\varepsilon_1}}{\kappa^2-1+e^{\frac{2}{C}\varepsilon_1}} \tag{A.9}$$

Substituting Eqs. (A.8) and (A.9) into Eq. (A.2), the burst failure condition becomes:

$$\left(\frac{\varepsilon_{1b}}{\varepsilon_{2b}}\right)^n = \frac{\kappa^2 e^{\frac{2}{C}\varepsilon_{1b}}}{\kappa^2-1+e^{\frac{2}{C}\varepsilon_{1b}}} \tag{A.10}$$

where ε_{2b} is related to ε_{1b} in Eq. (A.8). Thus, for a given value of n and κ, ε_{1b} can be solved from Eq. (A.10), and ε_{2b} is calculated from Eq. (A.8) with ε_{1b}. With the values of ε_{1b} and ε_{2b}, the exact solution of burst pressure can be determined from Eq. (23) or (25).

Appendix B. von Mises Flow Solution of Burst Pressure

This section analyzes the exact solutions of burst strains, burst stresses and burst pressure solution for the von Mises yield criterion (i.e., C = 2/√3), where the burst effective strains are obtained from Eqs. (A.8) and (A.10), the burst effective stresses are obtained from Eq. (9), and the burst pressure is obtained by integrating Eq. (23) or directly calculated from the power series solution in Eq. (28) (using the first ten terms) for different values of κ and n in terms of the von Mises criterion. The power series solution of burst pressure is then compared with the closed-from exact solution in Eq. (30) for the von Mises criterion to confirm the validity of this closed-form exact solution.

Figures B.1 and B.2 show the variations of von Mises burst strains ε_{1b} and ε_{2b} and von Mises burst stresses σ_{1b} and σ_{2b} with the diameter ratio of D_o / D_i, respectively, for five given strain hardening exponent values of n = 0.05, 0.10, 0.15, 0.20, and 0.25. Figure B.1 shows that 1) the two von Mises burst strains are nonlinearly related to D_o / D_i, 2) all ε_{1b} values are larger than the corresponding ε_{2b} values for a given n, and 3) all ε_{1b} values increase, but the corresponding ε_{2b} values decrease as D_o / D_i increases for a given n. Figure B.2 shows that 1) the two von Mises burst stresses are also nonlinearly related to D_o / D_i, 2) the von Mises burst stress σ_{1b} normalized by the true UTS increases with D_o / D_i for a given n, and 3) the normalized von Mises burst stress σ_{2b} decreases as both D_o / D_i and n increase. *Note that any of those von Mises burst strains or stresses can be used as a critical value in the strain or stress-based von Mises failure criterion to determine the burst pressure of a thick-walled pipe in an elastic-plastic FEA simulation.*

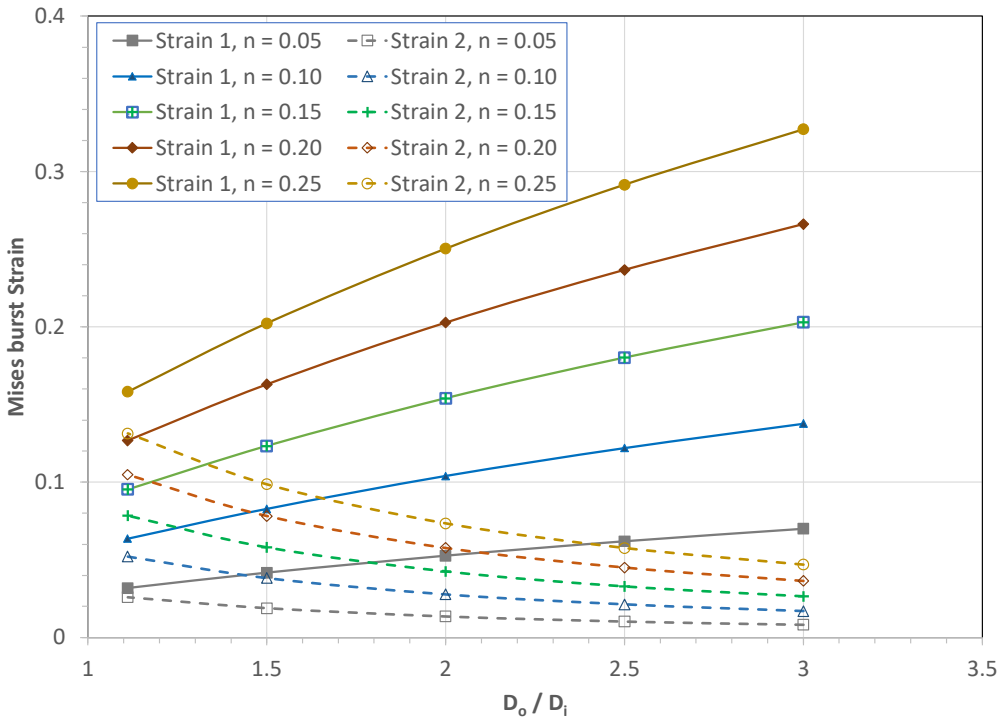

Figure B.1. Variation of von Mises strain at burst failure with D_o / D_i for five given n values.

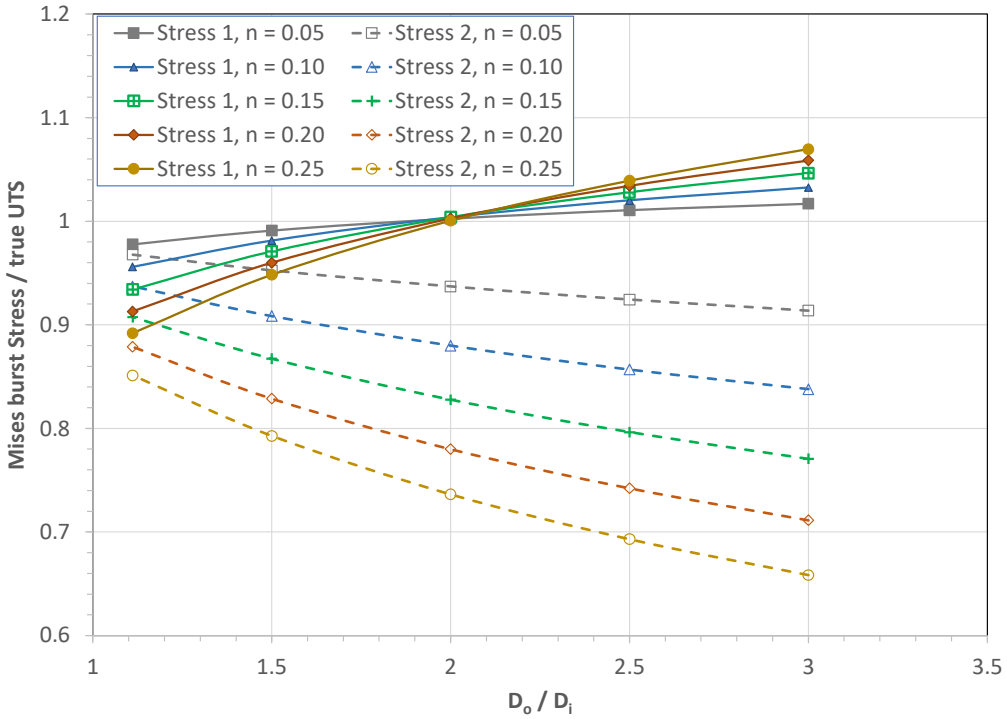

Figure B.2. Variation of von Mises stress at burst failure with D_o / D_i for five given n values.

Using the above determined values of von Mises burst strains ε_{1b} and ε_{2b}, the von Mises burst pressure is calculated directly from the power series solution in Eq. (28) with the first ten terms (or by integrating Eq. (23) with the trapezoidal rule and 50 equal incremental steps of integration). Figure B.3 depicts variations of the von Mises burst pressure ratio, $\frac{P_b}{S_{uts}}$, with the geometrical term $\ln\left(\frac{D_o}{D_i}\right)$ calculated from Eq. (28) for five given values of n = 0.05, 0.10, 0.15, 0.20, and 0.25. Also included in Fig. B.3 for comparison is the closed-form exact von Mises flow solution of burst pressure in Eq. (30), the Svensson approximate solution of burst pressure in Eq. (4), and the Svensson table data in Table 2 of Reference [21]. The comparison shows that 1) the present calculated burst pressure values are nearly identical to the Svensson table data for all n values, 2) the proposed von Mises flow solution in Eq. (30) agrees well with the calculated data, and 3) the approximate Svensson solution is always less than the calculated data or the proposed Mises flow solution for all n and all D_o / D_i ratios. From these observations, it can be concluded that 1) the proposed von Mises flow solution in Eq. (30) is a closed-form exact solution of burst pressure for thick-walled pipes, 2) the approximate Svensson model predicts a less non-conservative burst pressure in comparison with the exact Mises burst solution for a thick-walled pipe, and 3) the proposed integral equation (23) and the power series solution in Eq.

(30) using the second Bernoulli numbers both are validated by Svensson [21] when the von Mises yield criterion is adopted.

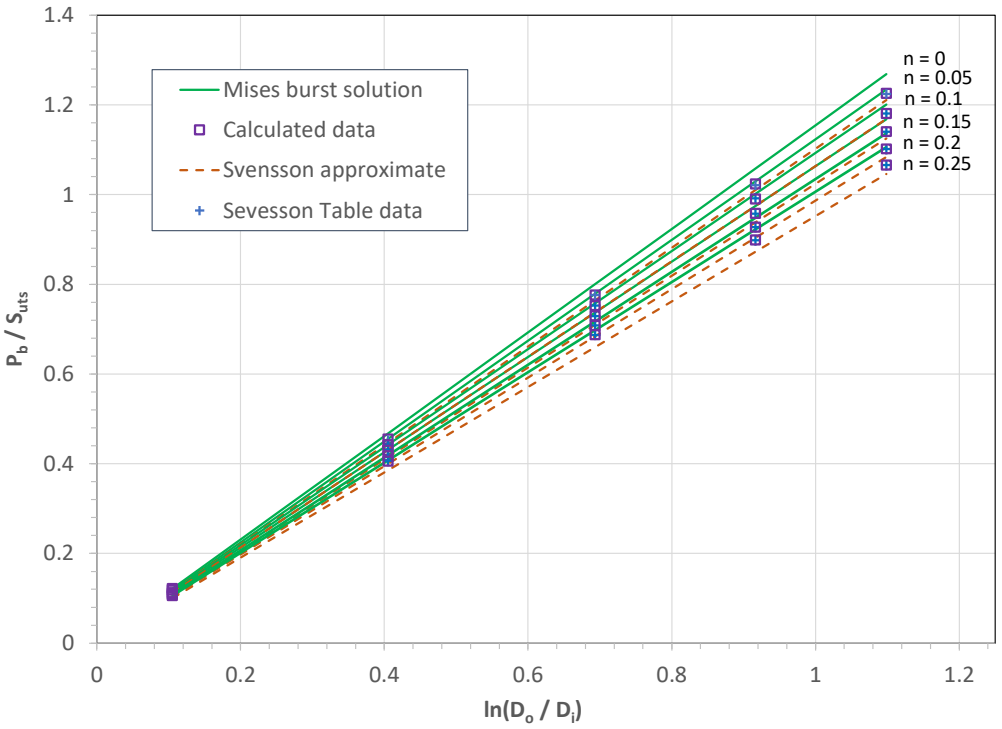

Figure B.3. Mises burst pressure ratio $\frac{P_b}{S_{uts}}$ against $\ln(D_o / D_i)$ for five given n values.

Appendix C. Tresca Flow Solution of Burst Pressure

This section analyzes the exact solutions of burst strains, burst stresses and burst pressure solution for the Tresca yield criterion (i.e., C = 1), where the burst effective strains are obtained from Eqs. (A.8) and (A.10), the burst effective stresses are obtained from Eq. (9), and the burst pressure is obtained by integrating Eq. (23) or directly calculated from the power series solution in Eq. (28) (using the first ten terms) for different values of κ and n in terms of the Tresca criterion. The power series solution of burst pressure is then compared with the closed-from exact solution in Eq. (30) for the Tresca criterion to confirm the validity of this closed-form exact solution.

Figures C.1 and C.2 show the variations of Tresca burst strains ε_{1b} and ε_{2b} and Tresca burst stresses σ_{1b} and σ_{2b} with the diameter ratio of D_o / D_i, respectively, for five given strain hardening exponent values of n = 0.05, 0.10, 0.15, 0.20, and 0.25. Figure C.1 shows that 1) the two Tresca burst strains are nonlinearly related to D_o / D_i, 2) all ε_{1b} values are larger than the corresponding ε_{2b} values for a given n, and 3) all ε_{1b} values increase, but the corresponding ε_{2b} values decrease as D_o / D_i increases for a given n. Figure C.2 shows that 1) the two Tresca burst

stresses are also nonlinearly related to D_o / D_i, 2) the Tresca burst stress σ_{1b} normalized by the true UTS increases with D_o / D_i for a given n, and 3) the normalized Tresca burst stress σ_{2b} decreases as both D_o / D_i and n increase.

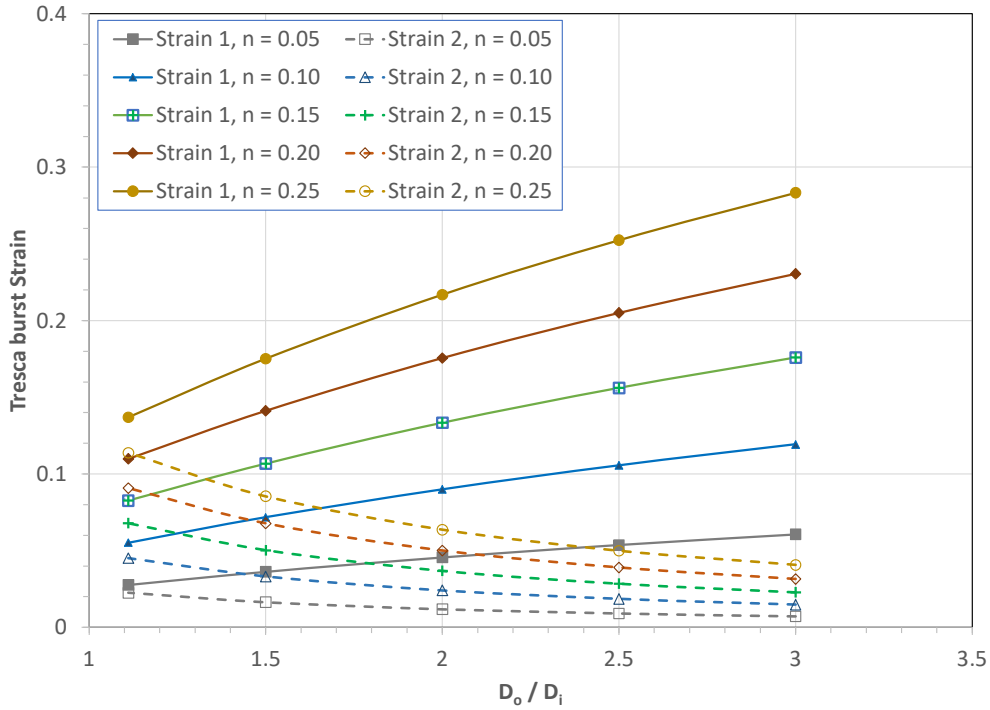

Figure C.1. Variation of Tresca strain at burst failure with D_o / D_i for five given n values.

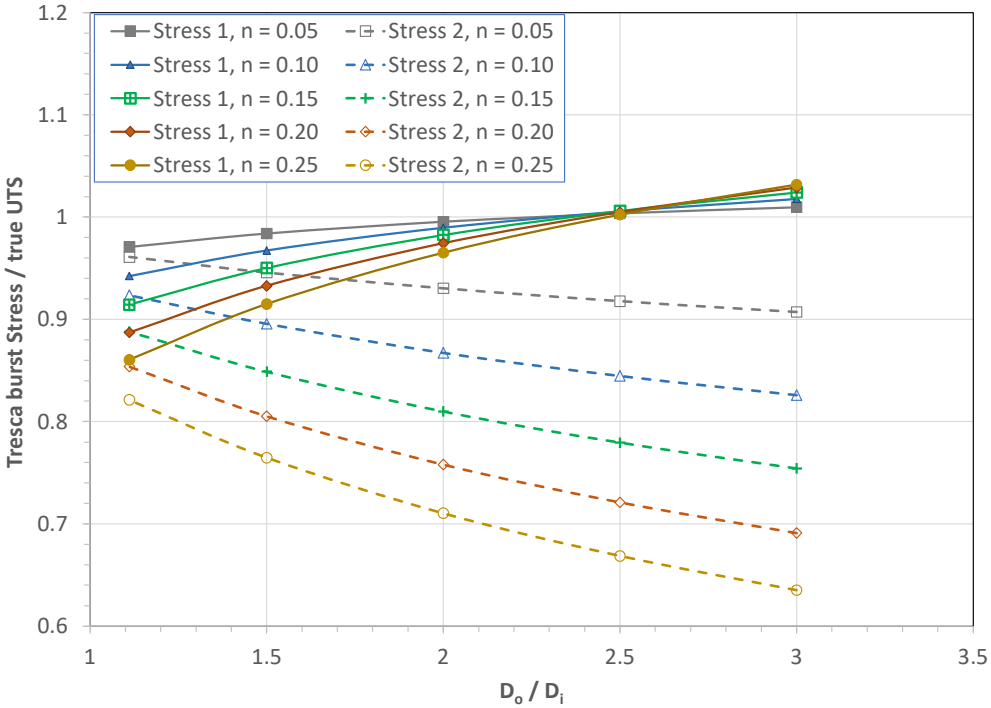

Figure C.2. Variation of Tresca stress at burst failure with D_o / D_i for five given n values.

Using the above determined values of Tresca burst strains ε_{1b} and ε_{2b}, the Tresca burst pressure is calculated directly from the power series solution in Eq. (28) with the first ten terms (or by integrating Eq. (23) with the trapezoidal rule and 50 equal incremental steps of integration). Figure C.3 depicts variations of the Tresca burst pressure ratio, $\frac{P_b}{S_{uts}}$, with the geometrical term $\ln\left(\frac{D_o}{D_i}\right)$ calculated from Eq. (28) for five given values of n = 0.05, 0.10, 0.15, 0.20, and 0.25. Also included in Fig. C.3 is the closed-form exact Tresca flow solution of burst pressure in Eq. (30) for comparison. The comparison shows that the proposed Tresca flow solution in Eq. (30) agrees well with the calculated data for all n values. From this observation, it can be concluded that the proposed Tresca flow solution in Eq. (30) is also a closed-form exact solution of burst pressure for thick-walled pipes when the Tresca yield criterion is adopted.

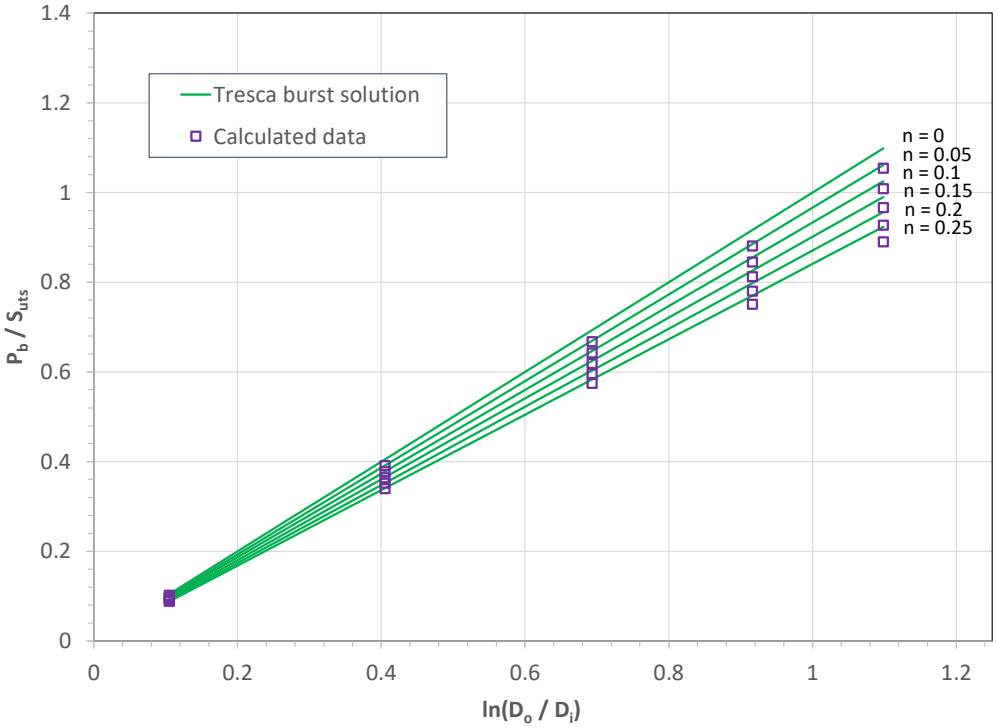

Figure C.3. Tresca burst pressure ratio $\frac{P_b}{S_{uts}}$ against $\ln\left(\frac{D_o}{D_i}\right)$ for five given n values.

International Journal of Mechanical Sciences

Ref. **Exact Solution of Burst Pressure for Thick-Walled Pipes Using the Flow Theory of Plasticity**
By Xian-Kui Zhu

Graphic abstract

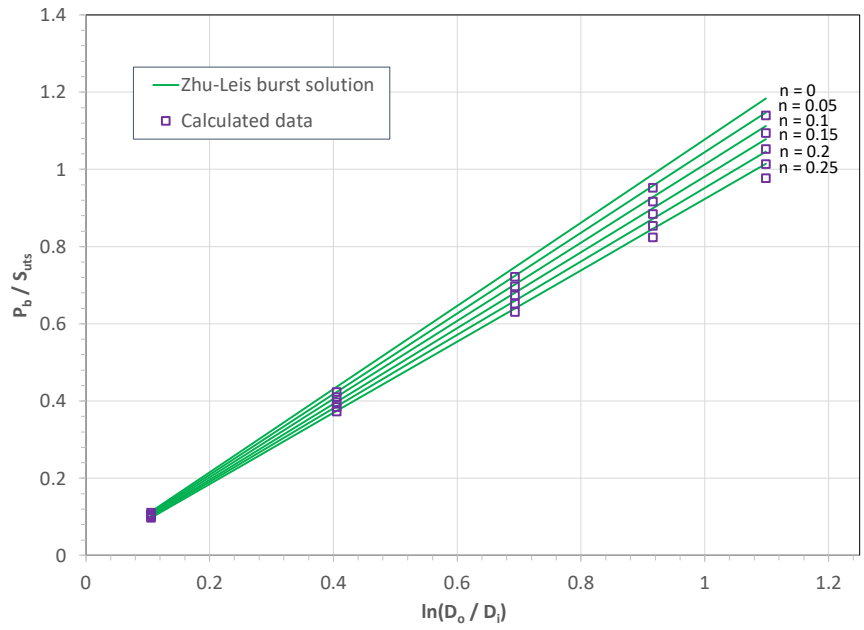

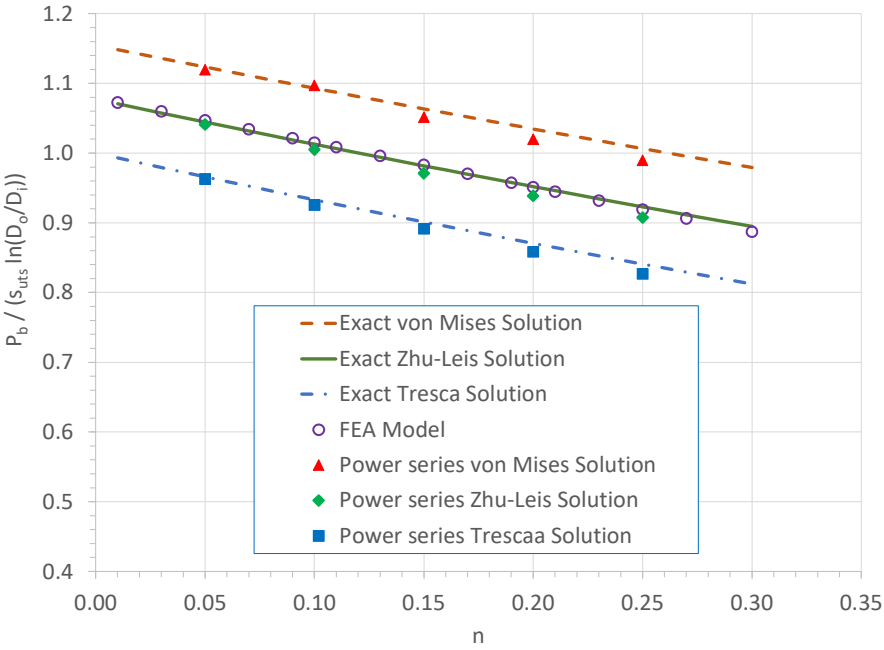

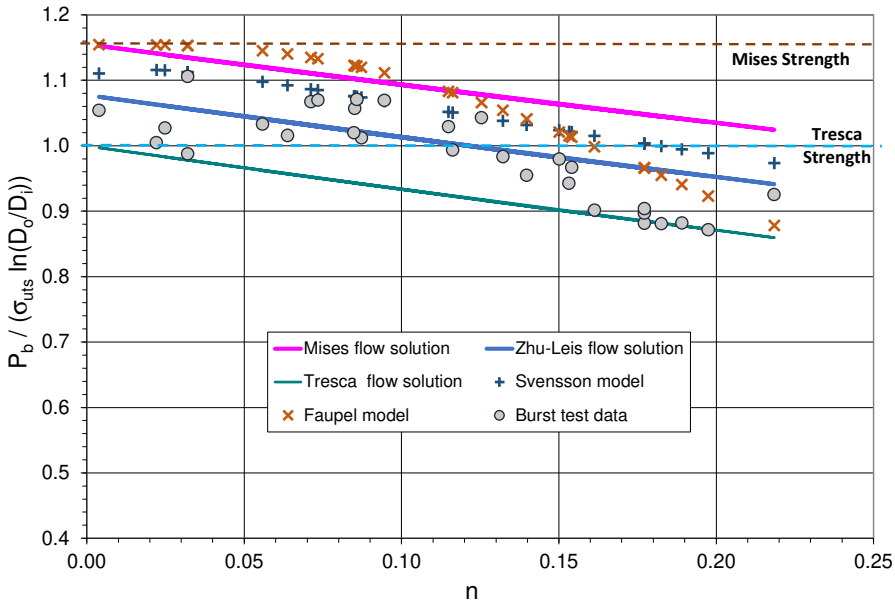
1.2
1.1
1.0
0.9
0.8
0.7
0.6
0.5
0.4
0.00
0.05
0.10
0.15
0.20
0.25
n
$P_b / (\sigma_{uts} \ln(D_o/D_i))$
Mises Strength
Tresca Strength
Mises flow solution
Zhu-Leis flow solution
Tresca flow solution
Svensson model
Faupel model
Burst test data